A CFD Investigation of Morphing Wing Configurations on a Submersible, Unmanned, Aerial, Vehicle Concept

Undergraduate Thesis

Presented in Partial Fulfillment of the Requirements for
Graduation with Distinction in the
Department of Mechanical and Aerospace Engineering
at The Ohio State University

by

Austin Spencer Petsche

May 2018

Advisor: Clifford A. Whitfield, Ph.D.

Defense Committee:

Richard Freuler, Ph.D.

Abstract

In 2008, the Defense Advanced Research Projects Agency, the central research and development organization for the United States Department of Defense, released a challenge for designers to create a vehicle that both flies and operates underwater. With the intent of reaching a target quickly and stealthily, the proposed mission focused on combining medium-altitude flight, low-altitude flight, and underwater navigation capabilities into a single entity. Medium-altitude flight would allow the vehicle to approach its target quickly. Low-altitude flight would allow the vehicle to get close to its target by hiding behind the curvature of the earth, effectively blocking radar and direct line-of-sight detection. And lastly, underwater navigation would enable the vehicle to get even closer to its target and to loiter in an area undetected.

Due to the varying atmospheric densities and the influence of the ground effect phenomenon, this research focused on the wing design for a submersible unmanned aerial vehicle concept. The trade study concentrated on the configuration and aspect ratio design of a wing capable of optimum performance in both medium-altitude and low-altitude flight conditions. Morphing wing configurations with variable wing sweep and variable wing anhedral were analyzed for their potential to meet desired performance characteristics in both the cruise and skim flight conditions. Although the morphing wing configurations tested proved adequate, a fixed, Reverse Delta wing with 10□ anhedral configuration at an aspect ratio of 3.37 was identified as having the ideal characteristics for optimum performance in each flight mode. The computational fluid dynamics software, XFLR5, provided the lift coefficient and moment coefficient data used to evaluate each wing configuration. This study provided evidence that combining vehicle abilities at differing flight altitudes is possible and can equip aircraft with more effective methods for achieving low observability states.

Table of Contents

List of Figures

List of Tables

Nomenclature

Symbols

AR	Aspect Ratio
b	Wingspan
c	Wing Chord
C_L	Lift Coefficient
L	Lift
ρ	Density
S	Wing Surface Area
V	Flight Velocity
W	Aircraft Weight

Abbreviations

Alpha	Angle of Attack
AoA	Angle of Attack
AR	Aspect Ratio
CFD	Computational Fluid Dynamics
CL	Lift Coefficient
ft	Feet
kts	Knots
mph	Miles Per Hour
RFP	Request for Proposal
RFS-1	Reid Flying Submarine Dash-1 Design
sq	Square
SUAV	Submersible Unmanned Aerial Vehicle
T/W	Thrust-Loading
W/S	Wing-Loading

Acknowledgements

I would like to thank my research professor and mentor, Dr. Clifford A. Whitfield, for the opportunity to learn and explore my passion of aircraft design. It was his teachings, guidance, and patience that truly cultivated my curiosity for aviation, inspiring boundless ideas and providing countless words of wisdom for overcoming life's challenges. I cannot put into words the appreciation I have for all of the time and effort he dedicated to my development as an engineer and as a person.

I would also like to thank Dr. Richard Freuler for taking the time to read this gruelingly long undergraduate research paper. With a mountain of work already on his desk, he took the time out of his busy schedule to serve on my defense committee and offer valuable, constructive criticism to further advance my scholastic abilities.

And lastly, I would like to thank my mom and dad. If it were not for their unyielding encouragement and support, I would never have gotten through an aerospace engineering program, let alone been able to write an undergraduate research thesis. They continue to motivate and inspire me to accomplish immeasurable feats and for that, I am most grateful.

Chapter 1: Introduction

1.1 Background

Since the inception of international conflict, knowledge has always bestowed its bearer with a competitive advantage. Whether it be the identification of enemy troops or insight into secret foreign technology, information has proven to be a priceless commodity during times of conflict. In many situations, this type of critical information is not readily presented by the opposition and thus, must be discretely obtained. Spies, drones, and reconnaissance vehicles are a few of the methods in which nations obtain secrets of adversaries. The key factor to each of these information attainment methods is the ability to remain undetected through the employment of stealth. Stealth can be broken down into a multitude of categories, tricks, and trades. However, there are four main classes of stealth technology universally recognized by the defense community: acoustic, infrared, radar, and visibility. Stealth technology in the visibility sector includes the employment of camouflage and direct line-of-sight avoidance methods. This research focused on combining two very different direct line-of-sight avoidance methods, ground-effect flight and underwater navigation. Ground-effect flight enables the vehicle to approach its target quickly and undetected by shielding the vehicle behind the curvature of the earth. The operation of a vehicle underwater reduces its ability to be visually detected from the surface and allows it to get even closer to its target. By combining these line-of-sight avoidance methods, a submersible unmanned aerial vehicle (SUAV) capable of attaining a new, heightened level of stealth could be created.

Conveniently bordered by bodies of water, the United States of America, like most privacy-seeking homeowners, enjoys a comfortable cushion between its coasts and those of its foreign neighbors. As delightful as this luxury may be, it does come at a price. As turmoil and controversy erupt overseas, the United States has a bit of a distance to travel in order to collect up-to-date information and to stay in the international loop. This lengthy distance across the Pacific Ocean hinders the United States' ability to react quickly to events that may arise in these foreign nations. Thus, presenting the need for a fast, on-

station, reconnaissance vehicle capable of deploying at a moment's notice while remaining under-the-radar and undetected.

Two tactics that avoid direct line-of-sight detection by an enemy are low-altitude flight and operation underwater. Low-altitude flight entails flying mere feet above a surface in order to utilize the curvature of the earth to hide from an opponent. It is similar to hiding from a pursuer on the other side of a hill, except in this case, the pursuer is much further away and the hill has significantly less height. Figure 1 shows an aircraft avoiding a radar line by utilizing low-level flight and the curvature of the earth.

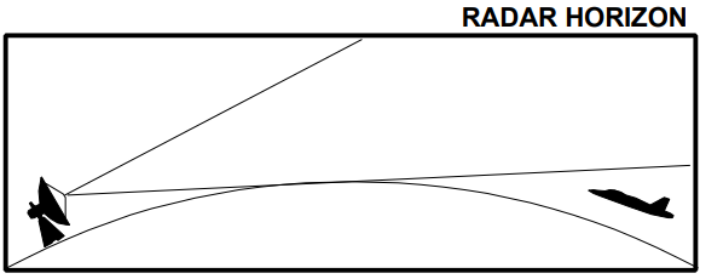

Figure 1: Radar Horizon [1]

Figure 2 exhibits a common practice nomogram used for determining the maximum distance an adversary can be from its target before the curvature of the earth no longer blocks radar signals.

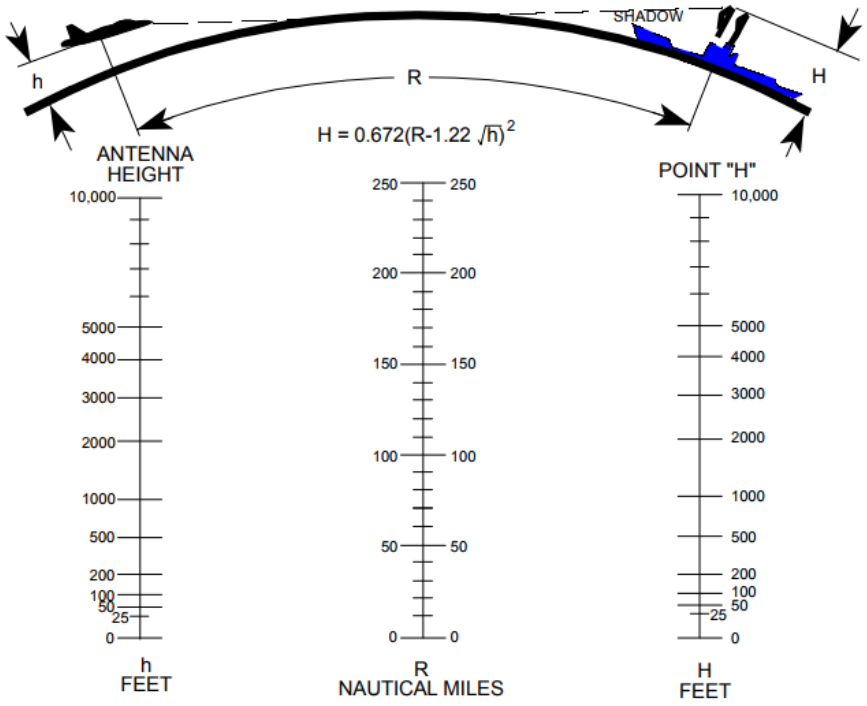

Figure 2: Earth Curvature Nomogram [1]

Interestingly, there are added benefits to low-level flight aside from those of stealth. In low-level flight, a phenomenon known as *ground effect* is employed. An aircraft creates lift from its wings because air travels faster over the top surface of the wing relative to the slower moving air on the bottom surface of the wing. The faster moving air on the top of the wing creates a low-pressure region relative to the high-pressure region created by the slower moving air beneath the wing. Figure 3 exhibits the pressure regions and flow speeds created by an airfoil.

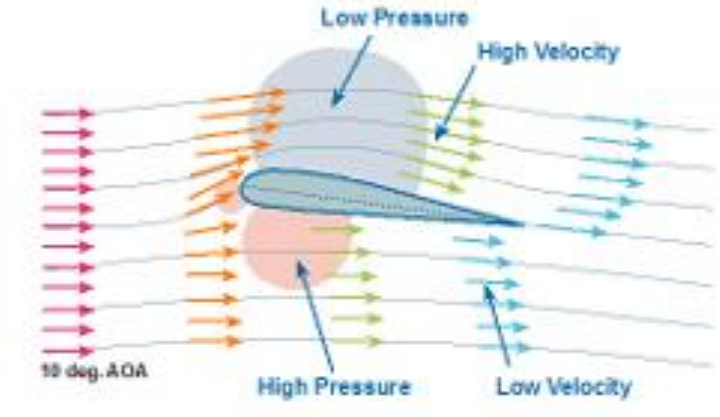

Figure 3: Airfoil Flow Velocities and Pressure Regions [2]

This pressure differential is what creates lift. It can be thought of as if the high pressure is what pushes the wing upward.

Near the tip of the wing, the high-pressure region leaks into the low-pressure region and creates wingtip vortices. These wingtip vortices further attribute to the creation of induced drag. This induced drag reduces the lift of the aircraft. For an aircraft in ground effect, the small distance between the ground and the bottom surface of the wing restricts the high-pressure region beneath the wing from flowing around the tip of the wing into the low-pressure region above the wing. By restricting this overflow, decreasing the potential for a reduced pressure differential, and creating a bubble of trapped pressure beneath the wing, the aircraft experiences improved lift and decreased drag. This results in lower fuel consumption and increased payload-carrying capabilities. Figure 4 exhibits how the high-pressure region is restricted from leaking into the low-pressure region when the aircraft is close a surface and flying in ground effect.

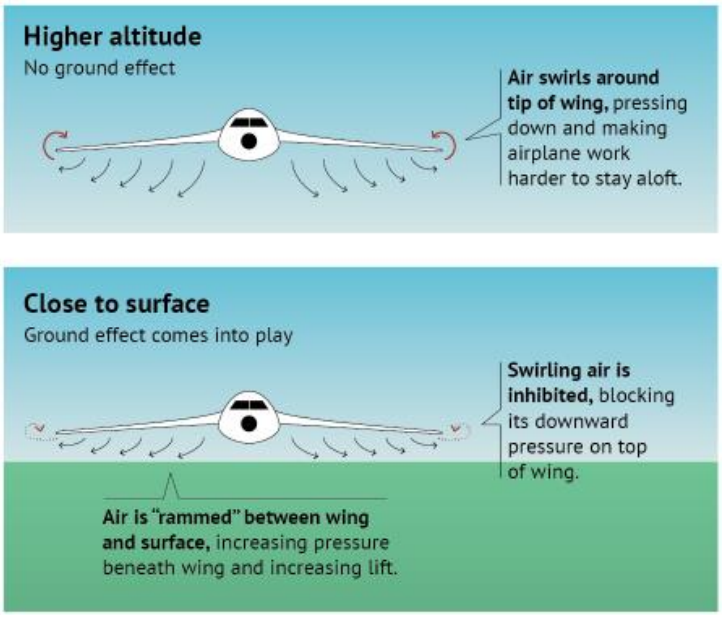

Figure 4: Ground Effect Phenomenon [3]

In addition to low-level flight, operation underwater also offers an advantage. By utilizing the cover of the ocean, vehicles that operate underwater not only avoid visual detection from entities above the surface of the water, but also render aircraft-detection radar ineffective due to the signal attenuation from the water. This allows the vehicle to get even closer to its target while still remaining undetected.

This research will focus on designing a quick-response, unmanned aircraft capable of accomplishing stealth-concentrated reconnaissance missions overseas. The aircraft will be capable of cruising at an altitude of 20,000 feet, flight in ground effect at altitudes of two to five feet above the surface of the water, also known as *skimming*, and have the ability to submerse and navigate underwater, similar to that of a submarine. Outfitted with reconnaissance equipment and an expendable payload, this aircraft will be launched from a catapult atop an aircraft carrier. By utilizing its unique methods of stealth, this aircraft will approach its target quickly and quietly to accomplish its mission. With the ability to loiter underwater, this SUAV will not only empower the United States to obtain information, but it will also provide the U.S. with the ability to deploy an expendable payload at a moment's notice should the situation necessitate.

1.2 Focus of Thesis

The purpose of this project was to develop initial design trade-studies for an aircraft capable of traversing through two different mediums, air and water. The majority of this research was dedicated to identifying a wing configuration and wing aspect ratio capable of optimum performance in both medium-altitude flight and low-altitude ground-effect flight. Using the computational fluid dynamics (CFD) program, XFLR5, the numerical computation and visualization software, MATLAB, and the solid-modeling computer-aided design program, SolidWorks, an initial conceptual design for an aircraft capable of medium-altitude flight, low-altitude flight, and underwater operation was created.

1.3 Significance of Research

To the public's knowledge, a submersible airplane or a flying submarine design has yet to be successfully created, tested, and developed on a high-volume scale. The inexistence of such a craft can be attributed to the fact that the drastic design requirements for submarines and aircraft are diametrically opposed. Aircraft are designed with weight minimization in mind, while submarines, on the other hand, necessitate heavy weights for submergence underwater. The differing environment mediums, air and water, contribute to dissimilar flow conditions along the vehicle and its lifting surfaces, therefore challenging the ability of the vehicle to achieve optimum performance in both modes. The structures of an aircraft and submarine also vary significantly. An aircraft structure is designed to act as a pressure vessel with minimal skin thickness, while submarine structures are designed with greater structures and skin thicknesses to resist the crushing loads of the sea. With larger structures, the weight of the submarine hinders the potential for flight. Furthermore, the wings and control surfaces of each craft can vary significantly. The lifting surfaces on a submarine, used for longitudinal control, are small in size since they are merely present to create relatively small forces to direct the craft. They are also located low on the submarine to ensure that even when surfaced, the lifting surfaces are submerged to enable the vehicle

to dive. Dissimilarly, the wings of an aircraft are long and have a large surface area to allow for the creation of lift. For amphibious aircraft, the wings are positioned high atop the vehicle to reduce the potential for contact with the water, hence the disparity between lifting surface size and location for aircraft and submarines. To further complicate the situation, the wings of a ground-effect vehicle are short in span and have an even greater surface area than medium-altitude aircraft. Therefore, to generalize this challenge, it is acknowledged that each vehicle has a different aspect ratio. An aspect ratio (AR) is a fraction relating the span and surface area characteristics of a wing. Equation 1[6] displays the aspect ratio relationship.

$$AR = \frac{b^2}{S} \tag{1}$$

Figure 5 provides a top view of the three types of aircraft to be combined. From the figure, it can be seen that the medium-altitude aircraft has a relatively high aspect ratio wing, while the ground effect aircraft and submersible vehicle have relatively low aspect ratio lifting surfaces.

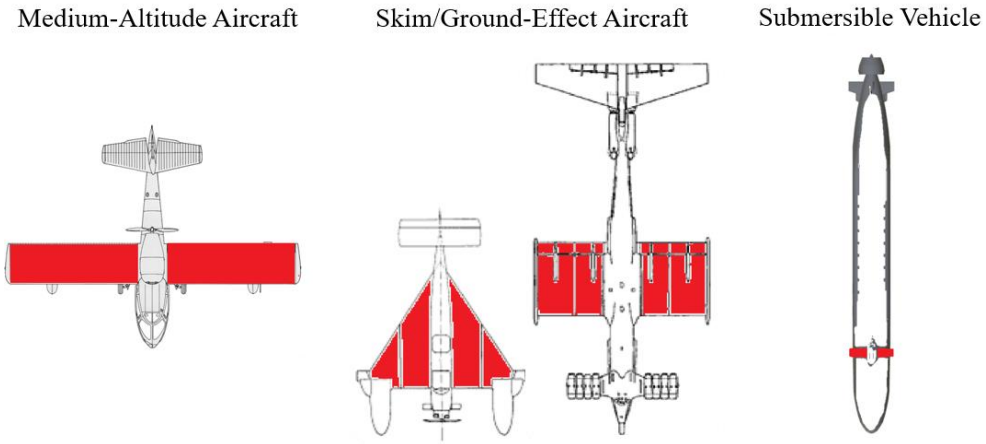

Figure 5: Wing shape and Aspect Ratio Discrepancy

Figure 5 highlights, in red, the discrepancy between each vehicle's lifting surface shape, size, and aspect ratio. Lastly, to add to the vehicle differences, aircraft engines and submarine engines vary in the fact that most aircraft power plants are lightweight and operate in an oxidizer-rich environment, whereas

submarine power plants must function independently of air or utilize a snorkel to achieve propulsion, neither of which prove to be light in weight.

There have been attempts by nations to accomplish this feat. In the 1930's, a design by Boris Ushakov was considered by the Russian military. The design saw much funding and interest, but for undisclosed reasons never went further than the research phase. Figure 6 displays Ushakov's design.

Figure 6: Russian SUAV Concept [4]

In the 1960's, Donald Reid's homebuilt design, the Reid Flying Submarine 1 (RFS-1), was constructed and marketed to the United States military. Unfortunately, the design did not see further development due to its lack of ability to sustain flight. Figure 7 displays the RFS-1 design.

Figure 7: Donald Reid's RFS-1 SUAV Concept [5]

In 2008, the Defense Advanced Research Projects Agency (DARPA), an American agency responsible for developing emerging technologies for the military, further reiterated the need for and the merit of such a vehicle by announcing its preparation to issue contracts for a submersible aircraft. The variety of attempts at designing such a vehicle and the competition initiated by the U.S. in 2008 exhibits the value militaries have placed on such capabilities.

With increased speed, enhanced range, and variable flight altitudes, the initial submersible aircraft design concept proposed in this research shows promise in exceeding the performance capabilities of previous designs and provides a feasible concept for further development. A unique feature of this craft is its wings. By creating a wing that functions optimally in both ground-effect flight and medium-altitude flight, the design experiences reduced fuel consumption, increased range, and increased speed in comparison to other SUAV designs.

This research is important because it both examines new wing configurations capable of optimum performance at drastically different flight altitudes and offers the United States a new vehicle concept capable of fast, on-station missions at sea.

1.4 Thesis Overview

This thesis has five chapters. The first chapter introduces the focus of this research and provides the reader with background information concerning the topic. The second chapter discusses the initial design process of the vehicle, highlighting initial weights and desired performance characteristics. The third chapter presents CFD wing configuration and aspect ratio trade studies to identify the ideal wing shape for the vehicle. The fourth chapter exhibits an initial conceptual design of the craft, providing a general layout and design renderings. The fifth and final chapter discusses the results of the wing-configuration trade study, examines the conceptual design presented, and proposes future direction for the research.

Chapter 2: Initial Design

2.1 Design Mission

To begin the design process, a mission first had to be established. With the intent of adhering to the customer constraints in the 2008 DARPA Submersible Aircraft Request for Proposal (RFP), the following mission was created. With the intent of creating a carrier-launched vehicle, the aircraft begins its mission by taking off from a 300-foot-long runway. From takeoff, it climbs to an altitude of 20,000 feet, where it quickly and efficiently cruises 500 nautical miles. When achieved, the vehicle descends to a height of approximately two to five feet above the surface of the water, where, with the help of ground effect, it skims 100 nautical miles to approach its target. At 600 nautical miles away from its runway, the aircraft descends from skim and lands on the water. Upon landing, the vehicle then begins the preparation process for underwater operation. When ready, the vehicle submerges underwater, and dives to the operational design depth. Once at depth, the SUAV cruises 16 nautical miles to its target, at which it can commence mission specific operations with the help of its advanced reconnaissance equipment and expendable payload. After loitering underwater for some time, the SUAV turns around and returns to its point of submergence, where a friendly vehicle retrieves it and brings it back it to base. Figure 8 is a pictorial representation of the design mission. Table 1 is an accompanying information relating the mission segments to their respective metrics.

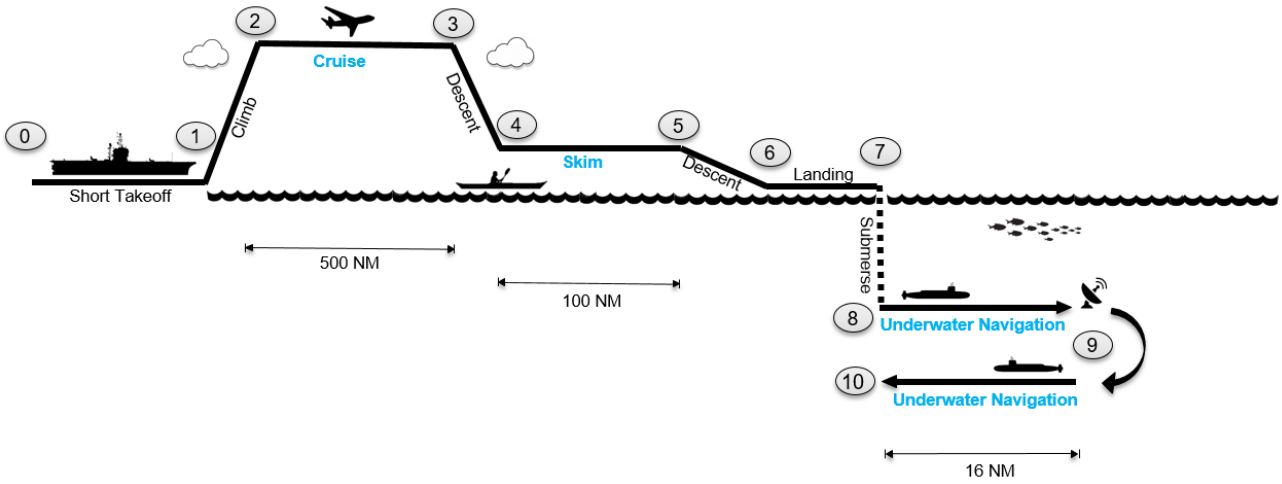

Figure 8: SUAV Mission Profile

Table 1: Mission Segment Metrics

Station	Mission Segment	Distance	Altitude
0-1	Warmup/Takeoff	>300 ft	
1-2	Climb		
2-3	Cruise out	500 NM	20,000 ft
3-4	Descent to skim		
4-5	Skim	100 NM	5 ft
5-6	Descent to landing		
6-7	Landing on water		Sea Level
7-8	Submerse		
8-9	Underwater Navigation to Target	16 NM	
9-10	Underwater Navigation return to submersion point	16 NM	

The respective metrics displayed in Table 1 are in compliance with the customer constraints specified in the 2008 DARPA RFP, *DARPA-BAA-09-06*. The cruise distance was the only value from the DARPA RFP that was shortened. The cruise distance was decreased to simplify the mission due to the time constraints of this undergraduate research.

2.2 Needs and Requirements

Next, the needs and requirements for the vehicle were established. By selecting the desired performance capabilities of the vehicle and correlating the specifications necessary to achieve the selected capabilities, a set of success criteria were identified for the focus of the design process. To correlate the necessary specifications to the desired performance capabilities specified in the DARPA RFP, a scoring process was executed. First, the desired performance capabilities of the vehicle, also referred to as the Needs of the vehicle, were ranked from one to five along the y-axis of the table, with the rank of five being the most important and the rank of one being the least important. Next, the necessary specifications were ranked from zero to nine along the x-axis of the table, with the rank of nine being the most necessary to meet the correlating desired performance characteristic. Once all specifications were ranked, each specification rank value of the rows was multiplied by the needs rank value in that row. Then the multiplied values within each specifications column were summed to achieve a total value. Finally, each total value was compared to the mean of all of the total values. The total values greater than the mean were identified as success criteria for this design challenge. The needs in the success criteria chart were identified as those listed with the highest rank, ranks of five. Table 2 shows the Needs Chart and how the success criteria were identified. Table 3 isolates the identified success criteria.

Table 2: Initial Design Needs Chart

Needs	Needs Importance (1-5)	Specifications: 500 NM cruise distance	100 NM skim distance	32 NM underwater navigation distance (round trip)	Loiter Speed (<= 130 knots)	Low landing speed (<= 83 knots)	Rapid descent to skim	Unrefueled Range > 700 NM	g-loads > 3	Specific Power (Ps) >= 0	Mach < 0.80 Cruise	Takeoff Distance < 300 ft (Carrier Launched)	Start - 10 lbs Fuel/Engine	Warmup - 20 lbs Fuel/Engine	Carry Expendable Payload	Underwater Survivability
Ship Launched	5	0	0	0	1	0	0	0	3	0	3	9	6	6	0	0
High Subsonic CRUISE (>= 333 knots)	5	9	0	0	9	6	6	9	9	9	9	6	3	3	1	0
Mid-High Subsonic SKIM (>= 200 knots)	5	0	9	0	6	9	6	9	6	3	1	6	1	1	3	0
Land on Water	5	0	0	1	3	9	0	1	1	0	0	6	0	0	1	1
UAV	5	1	1	1	3	1	1	0	0	0	0	3	0	0	1	6
Submerse Underwater	5	0	0	6	0	0	0	0	0	0	0	1	0	0	6	9
Mid-speed Navigation UNDERWATER	5	0	0	9	0	0	0	0	0	0	0	0	0	0	6	9
Sufficiently Affordable	2	6	6	6	3	3	3	6	6	3	6	6	3	3	6	6
Low Observability	4	9	9	6	1	3	6	6	0	0	6	1	0	0	0	9
Carry Flexible Payload (reconnaissance equipment & armarment)	4	0	0	1	6	1	0	1	0	1	1	0	0	0	9	6
Water Tight	4	0	0	9	0	6	0	0	0	0	0	0	0	0	3	9
Compatibility/integration with current systems	3	0	1	6	3	0	0	0	0	0	0	6	0	0	1	6
Reasonable fuel consumption	2	9	9	3	6	3	0	9	0	6	6	6	3	3	1	3
Mid-High Energy Maneuverability	4	0	0	0	3	3	6	0	9	9	6	1	0	0	1	0
Short Manufacture Time	1	0	0	3	0	0	0	0	1	0	0	0	0	0	0	3
Stable in Cruise and Skim	5	6	6	0	6	6	3	0	1	0	1	3	0	0	0	0
	TOTALS:	146	149	188	207	219	134	153	149	118	146	220	62	62	159	260
	Above Mean:	FALSE	FALSE	TRUE	TRUE	TRUE	FALSE	FALSE	FALSE	FALSE	FALSE	TRUE	FALSE	FALSE	TRUE	TRUE
	Mean:	158.133														

Table 3: Initial Design Success Criteria

SUCCESS CRITERIA	
NEEDS	**SPECIFICATIONS**
Ship Launched	32 NM underwater navigation distance (roundtrip)
High Subsonic CRUISE (>= 333 knots)	Loiter Speed (<= 130 knots)
Mid-High Subsonic SKIM (>= 200 knots)	Low landing speed (<= 83 knots)
Land on Water	Takeoff Distance (< 300 feet; carrier launched)
UAV	Carry Expendable Payload (= 600 lbs)
Submerse Underwater	Underwater Survivability
Mid-speed Navigation UNDERWATER	
Stable in Cruise and Skim	

From the Needs Chart and Success Criteria table, the desired performance specifications for the cruise and skim flight segments of the SUAV mission were identified. The desire performance specifications include the high subsonic flight speeds greater than or equal to 333 knots (383 mph) in cruise, the mid-high subsonic flight speeds greater than or equal to 200 knots (230 mph) in skim, the loiter speeds less than or equal to 130 knots (150 mph) in cruise, and landing speeds less than or equal to 83 knots (96 mph) in skim. These values were identified based off of the eight hour maximum total time to complete the mission requirement specified in the DARPA RFP.

2.3 Thrust-Loading and Wing-Loading Trade Study for Cruise Conditions

Thrust-loading (T/W) and wing-loading (W/S) are two of the fundamental characteristics in aircraft design. Both define and influence the overall performance of an aircraft. Following the selection of the desired performance metrics for the cruise and skim flight modes, a trade study was performed to identify how the thrust-loading and wing-loading values changed for an aircraft as certain characteristics were varied in the different flight conditions.

In cruise flight, increasing the aspect ratio (AR) of the wing induced an increase in the minimum wing-loading required for flight. This is because when the aspect ratio is increased and the weight of the vehicle is fixed, either the span of the wing increases or the surface area of the wing decreases, therefore increasing the value of the wing-loading. Figure 9 demonstrates this correlation.

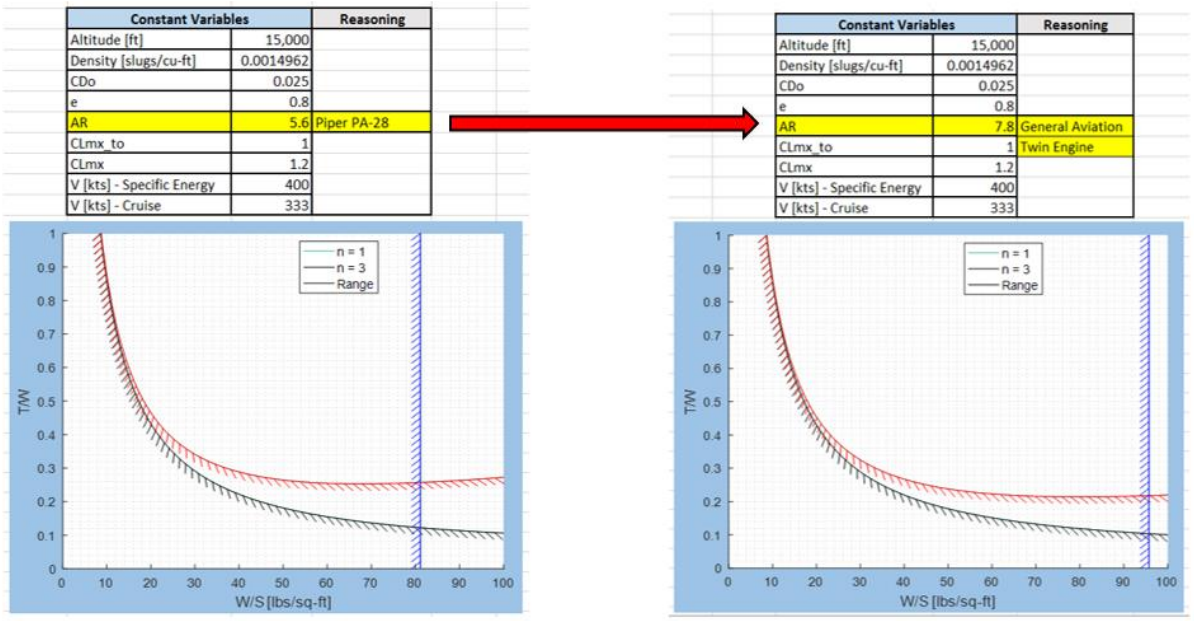

Figure 9: Aspect Ratio Influence in Cruise

When the altitude for cruise flight was increased, the minimum wing-loading required for flight was reduced. This was due to the fact that as altitude increases, the air becomes less dense. Additionally, increasing the flight altitude increased the thrust-loading required for higher gravity loading maneuvers. Figure 10 displays both results.

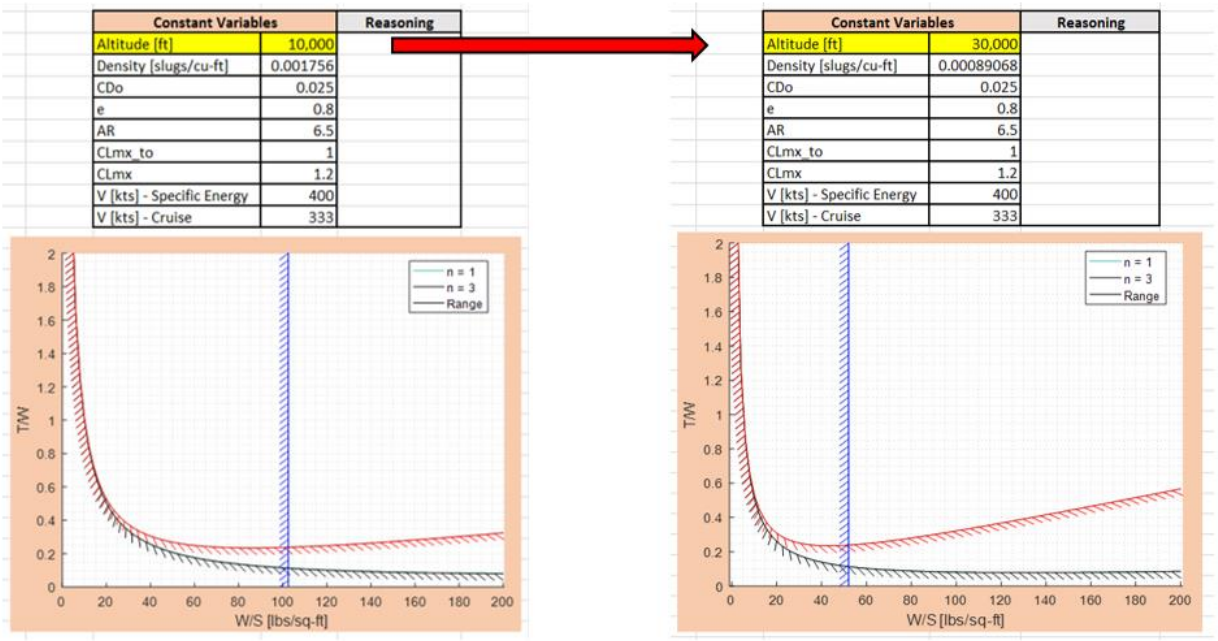

Figure 10: Altitude Influence in Cruise

Decreasing the flight velocity in the cruise condition, reduced the minimum wing-loading required of the aircraft, but also increases the thrust-loading necessary to perform rapid maneuvers at greater wing-loading values. Figure 11 exhibits this relationship.

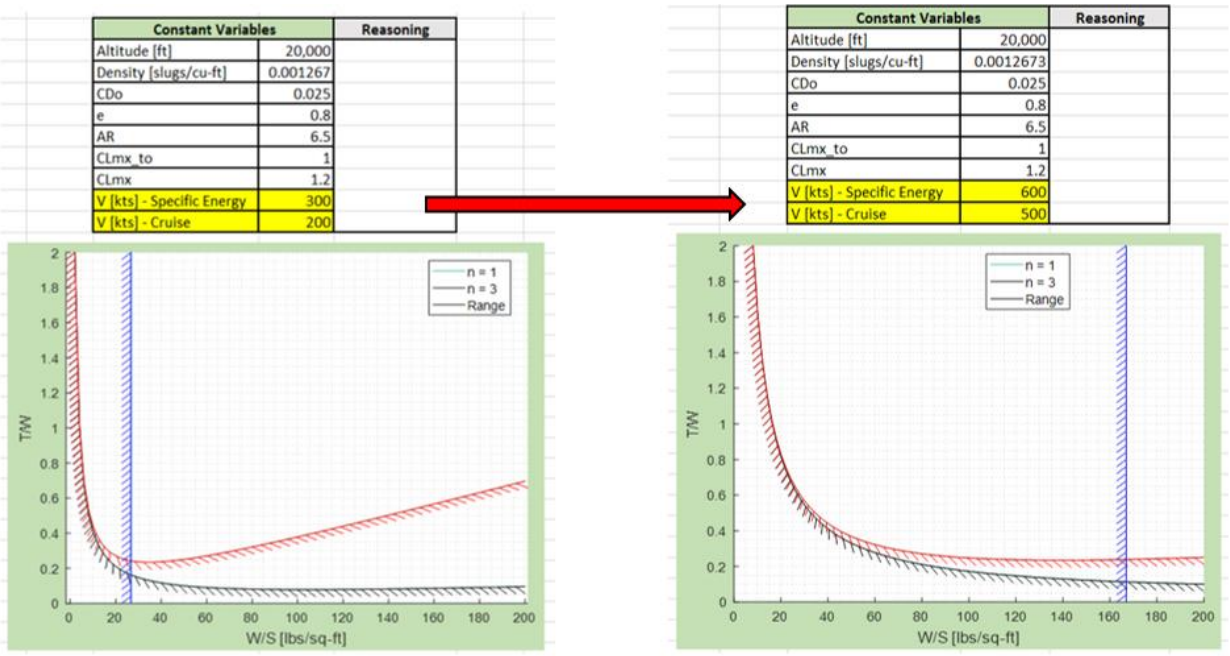

Figure 11: Flight Velocity Influence in Cruise

From this thrust-loading and wing-loading trade study for cruise conditions, initial cruise flight performance parameters were selected for the SUAV. Figure 12 defines the selected parameters.

Constant Variables		Reasoning
Altitude [ft]	20,000	
Density [slugs/cu-ft]	0.0012673	
CDo	0.025	
e	0.8	
AR	6.5	
CLmx_to	1	
CLmx	1.2	
V [kts] - Specific Energy	400	
V [kts] - Cruise	333	
Minimum T/W	0.2449	
Minimim W/S	74.05	

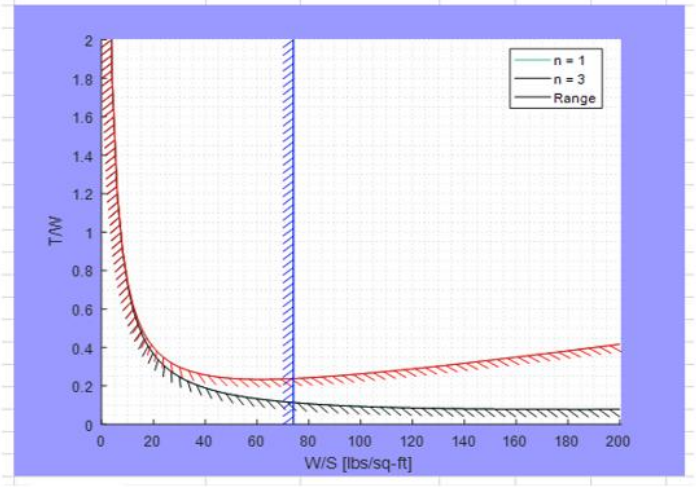

Figure 12: Ideal Performance Parameters for Cruise

2.4 Thrust-Loading and Wing-Loading Trade Study for Skim Conditions

Increasing the flight altitude does not change the wing-loading until about 5,000 feet, where the change in atmospheric density is more significant. Increasing the flight altitude changes the thrust-loading required for higher g-loading. However, the thrust-loading change only begins to be apparent starting at about 5,000-10,000 feet, where the atmospheric conditions begin to change more drastically. Figure 13 displays this relationship.

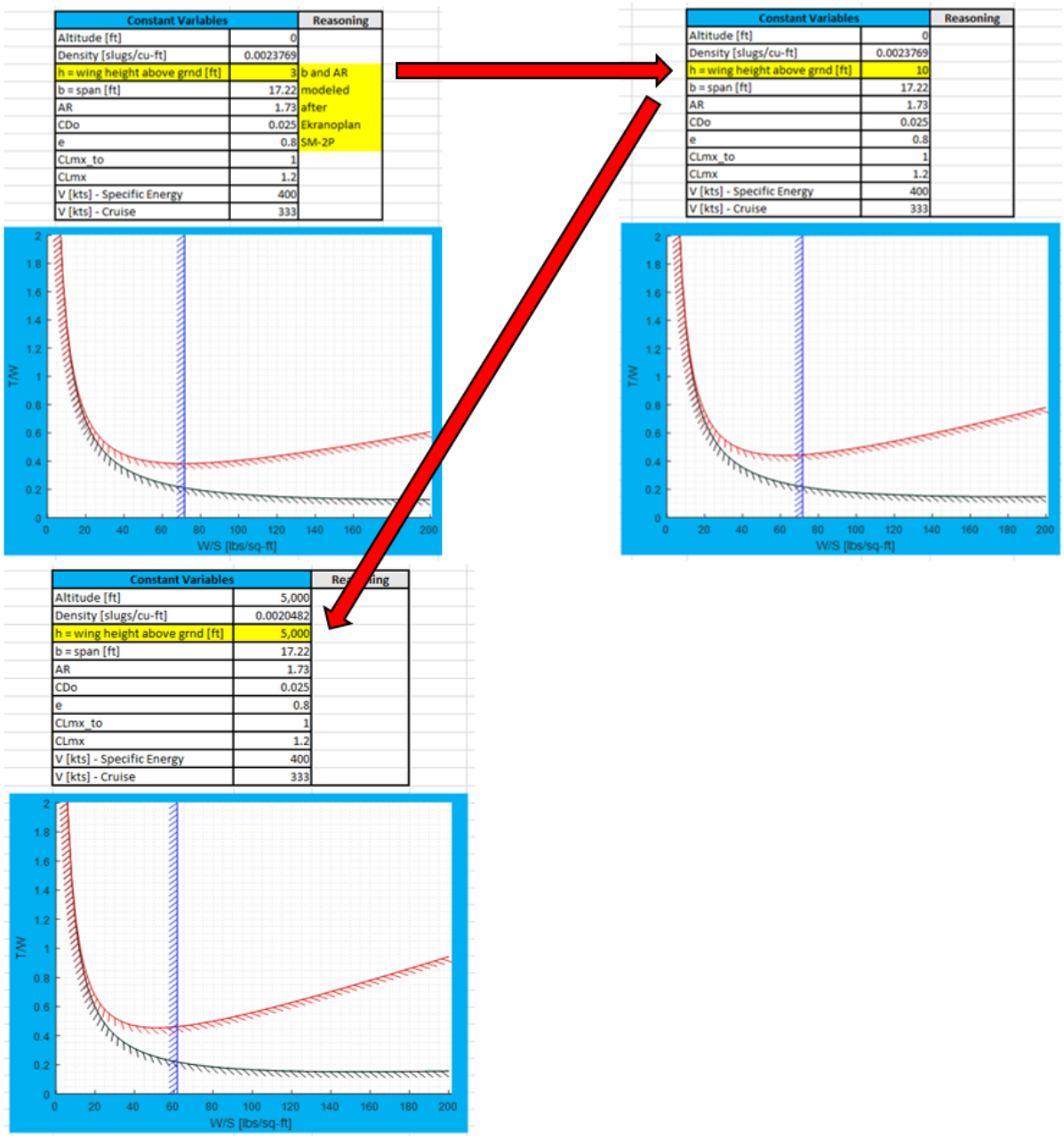

Figure 13: Ground Effect Height Influence in Skim

When the aspect ratio is increased in skim flight conditions, the minimum wing-loading required for flight is increased and the minimum thrust-loading required for maneuvering is decreased. Figure 14 provides a visual for this correlation.

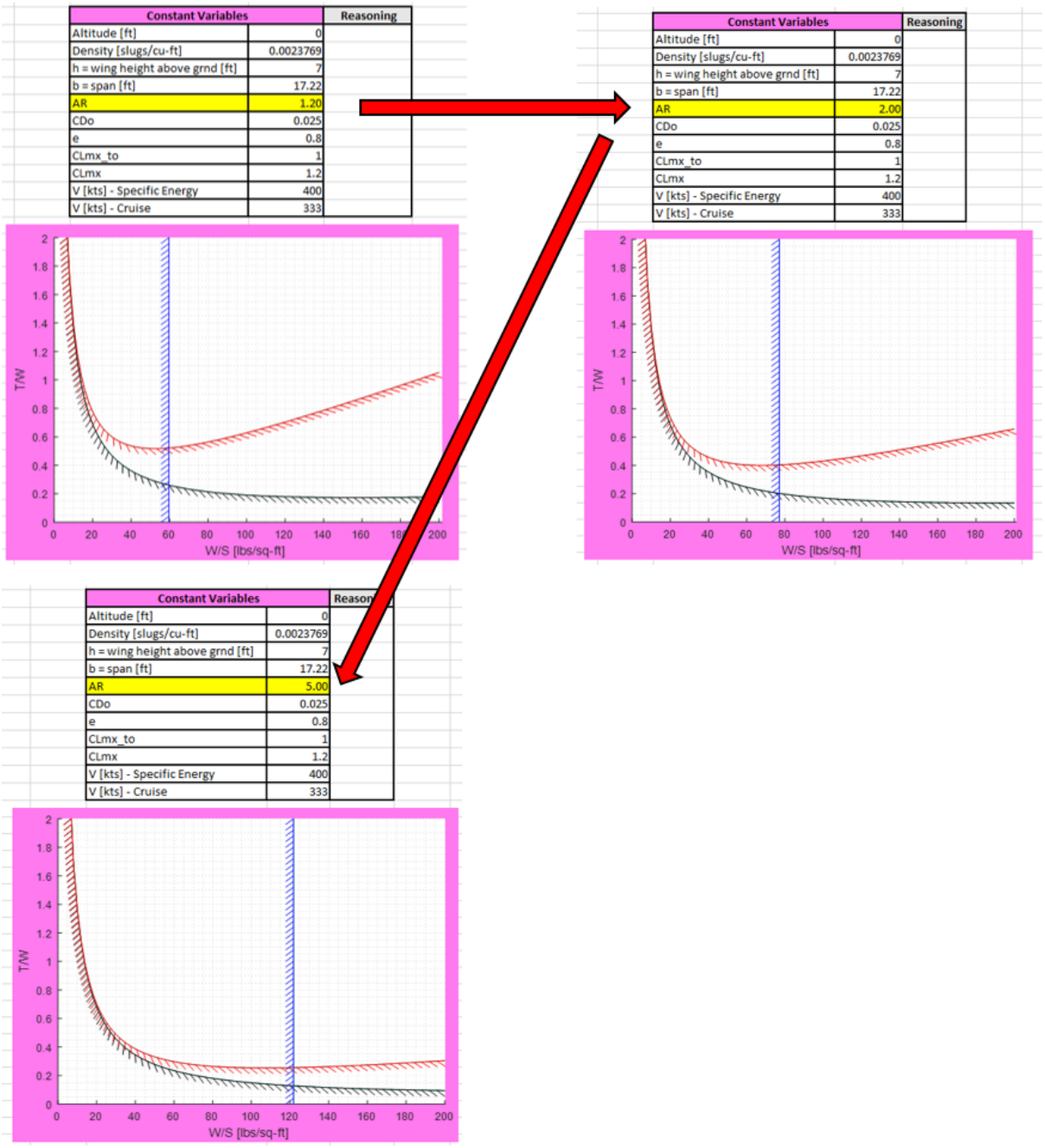

Figure 14: Aspect Ratio Influence in Skim

Increasing the wingspan of an aircraft in skim flight slightly reduces the minimum thrust-loading required for higher gravity maneuvers. Significant reductions in thrust-loading occur when the span reaches 50 feet or more. Figure 15 exhibits this relationship.

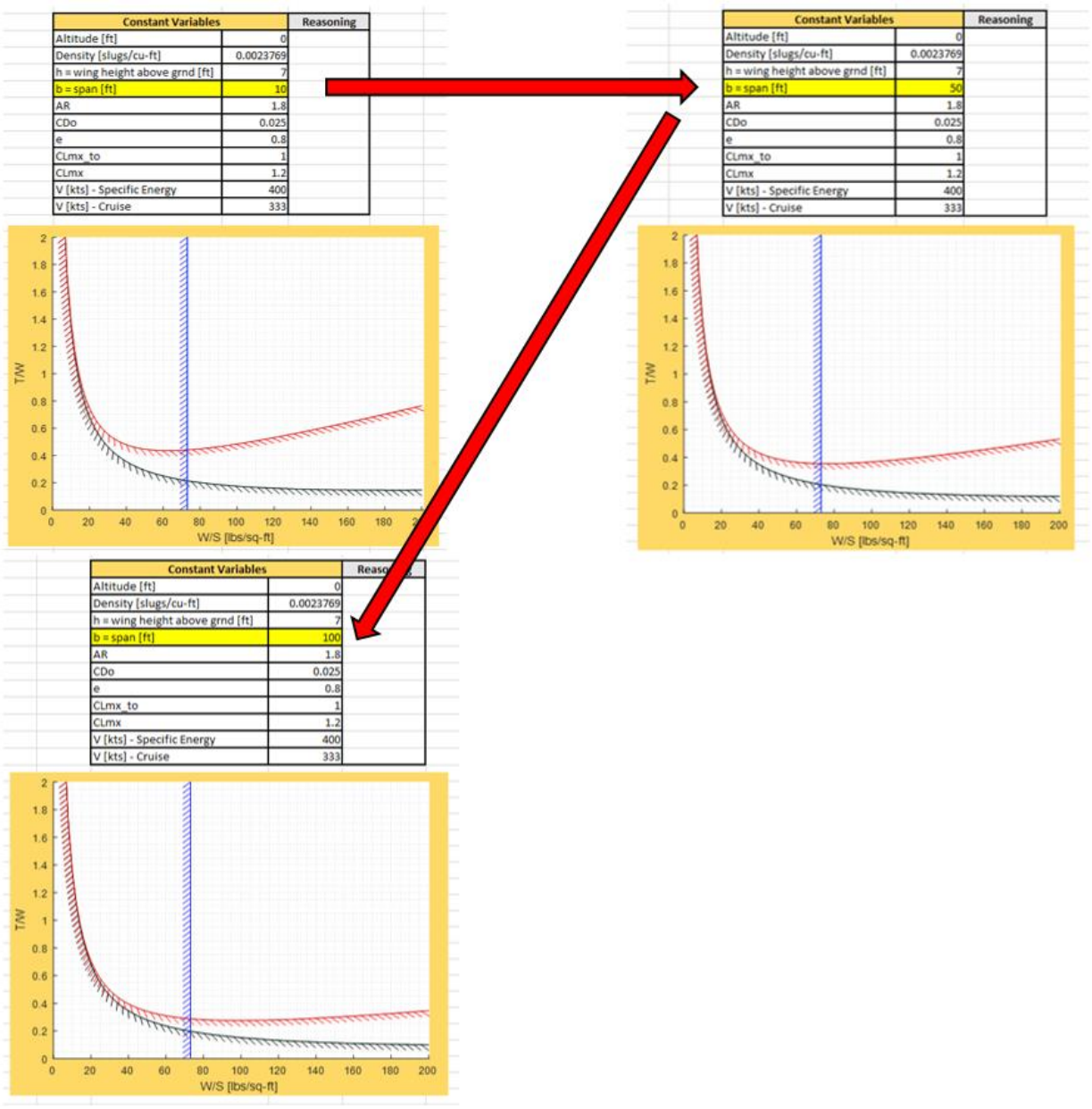

Figure 15: Wingspan Influence in Skim

These trade studies offered a general depiction of how aircraft characteristics influence the thrust-loading and wing-loading values for a vehicle. They also identified general metrics to select as initial testing values for the wing analyses to be performed in chapter three.

Chapter 3: Wing Configuration Trade Study

The first two mission segments for the SUAV include cruise flight at a medium-altitude height of 20,000 feet and skim flight at a low-altitude height of two to five feet. Due to the influence of ground effect during skim and the differing atmospheric densities at the mission segment altitudes, wing configurations designed to satisfy each of these flight conditions vary significantly. For that reason, the following trade study was performed to identify a wing shape and size that would perform optimally in both medium-altitude cruise flight and ground-effect skim flight. Both fixed and morphing wing configurations were analyzed.

3.1 Test Parameters

In order to isolate the parameters upon which to base this study, the following desired vehicle performance characteristics were established: high subsonic flight speeds in both cruise and skim to decrease the time to target, low stall speeds in skim for water landings, and low loiter speeds in cruise for surveillance operations and landing preparation. Equation 2[6] displays the general relationship between the variables affecting the flight performance of a wing in steady-level flight.

$$W = L = \frac{1}{2}\rho V^2 S C_L \tag{2}$$

By setting the lift (L) equal to the weight (W) of the aircraft for steady level flight, while keeping the atmospheric density (ρ), flight velocity (V), and wing reference area (S) constant, the only remaining variable influencing the performance of a wing is the lift coefficient (C_L). Although a multitude of factors contribute to the determination of the lift coefficient for a wing, the shape of the wing stands out as the most impactful factor during the conceptual design process. For that reason, wing configuration and aspect ratio, two factors that define the shape of a wing, were examined in this study. Wing configuration was analyzed first, as it provided the general trends for the achievable lift coefficients of each wing

concept. Once a configuration was established, the wing aspect ratio was investigated to attain a more accurate representation of the achievable lift coefficients.

In order to link the lift coefficient variable of the wing to our desired vehicle performance characteristics, the plots in Figure 16 and Figure 17 relating the design lift-coefficient to the forward flight velocity of the vehicle were created for both the cruise and skim mission segments. By comparing the lift coefficient data received from the Laplace equations used in XFLR5 computational fluid dynamics studies to these plots, vehicle performance characteristics were approximated.

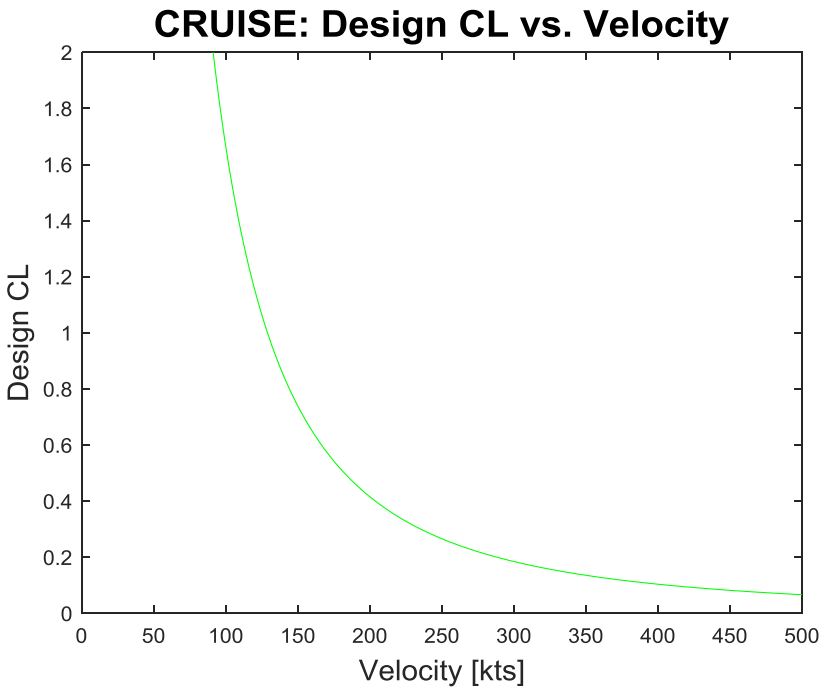

Figure 16: Lift Coefficient versus Flight Velocity Performance Map in Cruise

The lift coefficient versus velocity plot for the cruise situation shows that in order to attain a high flight speed in cruise, a low lift coefficient is required. Ideally, the low lift coefficient would be experienced at a zero to low angle of attack. This would allow for a greater range of angles of attack to be used to achieve the higher lift coefficients necessary for slower speed landing operations.

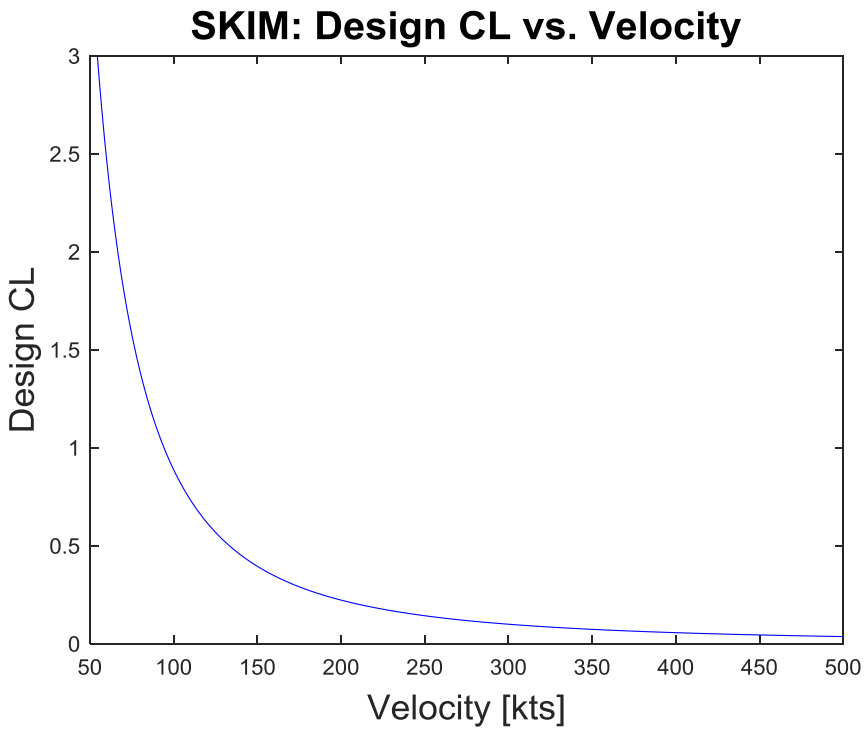

Figure 17: Lift Coefficient versus Flight Velocity Performance Map in Skim

Figure 17 portrays the lift coefficient versus velocity relationship for the skim flight conditions. Similar to the relationship in the cruise flight condition plot, a low lift coefficient is required to achieve high velocity flight in skim and a high lift coefficient is required to achieve low velocity flight in skim. Therefore, from Figure 16 and Figure 17, it was determined that the ability of a single wing to achieve high and low lift coefficients in both flight conditions is necessary to achieve the desired performance characteristics established for the SUAV.

Additionally, it was discovered that increasing the wing-loading (W/S) of the aircraft moved the entire dataset trend line for both flight conditions to the right, consequently increasing the minimum velocity attainable and increasing the lift coefficient required to achieve the higher minimum flight velocities. Figure 18 exhibits this relationship.

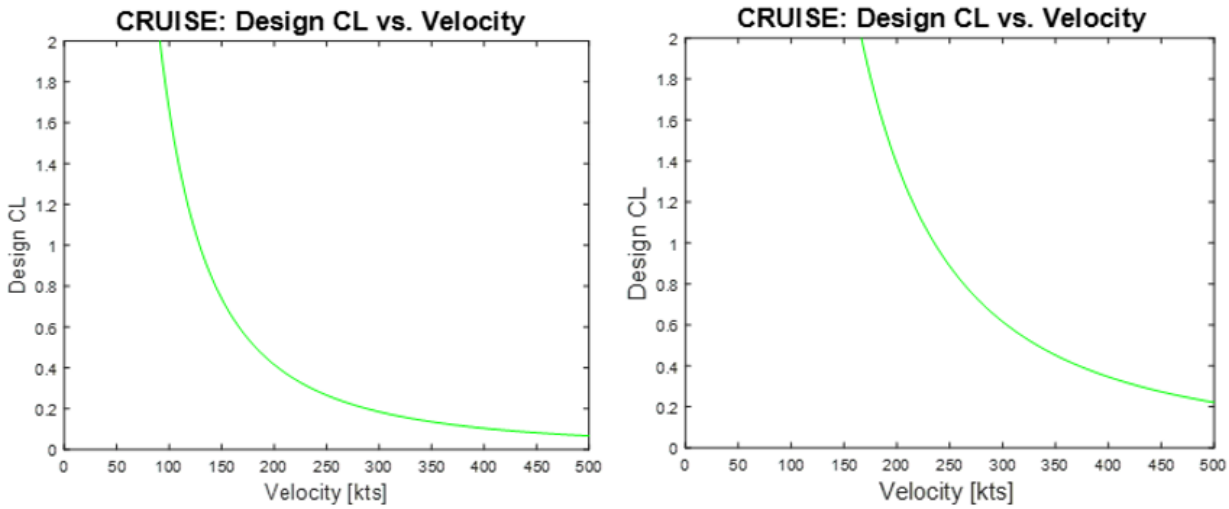

$W/S = 30\ lbs/(ft)^2$ $W/S = 100\ lbs/(ft)^2$

Figure 18: Wing-Loading Lift Coefficient Comparison in Cruise

With the lift coefficient and flight velocity relationship established for both cruise and skim, the wing configurations were then judged for their suitability to meet the desired performance characteristics of the SUAV. In order to minimize the variables affecting the analysis of the wing, the following tools and test parameters were selected. The computational fluid dynamics software, XFLR5, was chosen to perform this study due to its availability and quick computational time. This low order solver is capable of performing large scale changing of models in an efficient manner and a short amount of time due to its panel method approach. To model both cruise and skim, three flight conditions were tested: cruise flight at 20,000 feet, sea level skim flight at five feet in ground effect, and sea level skim flight at two feet in ground effect. Since 333 knots was defined in the thrust-loading and wing-loading trade study as an ideal initial performance parameter for the SUAV, it was held constant for each flight mode tested. The Ring Vortex, noted as *Vortex Lattice Method 2* in XFLR5, with inviscid conditions was used for this analysis. The angle of attack of the wing was selected as the independent variable for the study and was analyzed from 0° to 15°. The accuracy of this low order solver to model the stall characteristics of the wing is not high. Therefore, the wing, without high-lift devices, was approximated to stall around a 15° angle of attack. Although the wings were analyzed at angles of attack up to 15°, each lift coefficient plot depicts

the lift curve slope up to 20° angle of attack. The higher angles of attack offer an idea of potential performance capabilities of each wing configuration with the influx of high-lift devices. This information was helpful in understanding minimum achievable landing speeds, a parameter that is directly proportional to high lift coefficients.

This method of analysis generalized the trends of the lift coefficients achievable at these flight altitudes. It showed which wing configurations had higher or lower lift coefficient values at each flight condition with respect to their angle of attack. Once these trends were identified, they were referenced to Figure 16 and Figure 17 to approximate what speeds and performance qualities they were capable of achieving based off of the obtained lift coefficient values. With this information, the ideal wing configuration was determined and an aspect ratio trade study was begun. The aspect ratio study was performed to identify what aspect ratio value for the identified wing configuration would deliver values closest to the desired performance characteristics of the SUAV. The final wing, from the configuration and aspect ratio trade studies, was then analyzed again in XFLR5 to achieve more accurate depiction of the achievable lift coefficients.

3.2 Test Reference Wings

In addition to defining the tools and test parameters for this study, a frame of reference had to be established for the expected performance of the wings in each flight mode. Therefore, wings traditionally used in medium-altitude flight and ground-effect flight were analyzed. For cruise conditions, the Rectangular style wing was selected as a reference wing due to its simplicity and conventional use at the 15,000-20,000 feet flight altitudes. For skim conditions, the Reverse Delta style wing with a 20□ anhedral was selected as a reference wing due to its popularity and proven success on ground-effect vehicles. Lastly, the low aspect ratio Delta style wing was selected because it modeled a wing shape used in both medium altitude and low altitude flight conditions. The low aspect ratio Delta wing is commonly

used in high speed, medium altitude flight and also resembles the ground-effect wing configuration known as an *Ekranoplan*. For consistency, each reference wing was built with the NACA 2415 airfoil. Figure 19 displays the three wings used for reference.

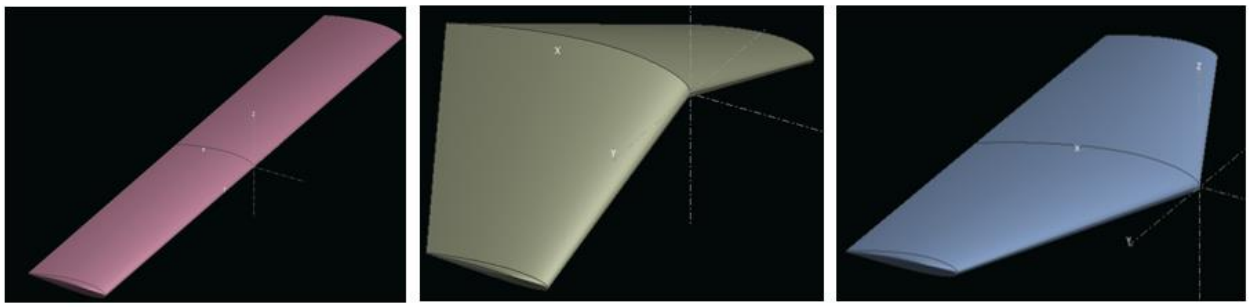

Figure 19: Reference Wings

After analyzing the three reference wings in XFLR5, Table 4 was created to display the resulting performance data. This table provided the lift coefficients experienced for each reference wing at the three flight conditions, cruise flight at an altitude of 20,000 feet, skim flight at an altitude of five feet, and skim flight at an altitude of two feet.

Table 4: Reference Wing Lift Coefficients

Coefficients of Lift for Reference Wings				
	Angle of Attack (degrees)	**CL @ Altitude: 20,000 ft**	**Cl @ Altitude: Sea Level (5 ft)**	**CL @ Altitude: Sea Level (2 ft)**
Rectangular	0^0	0.158	0.172	0.198
Reverse Delta (20^0 Anhedral)	0^0	0.116	0.126	0.268
Delta	0^0	0.118	0.124	0.141
Rectangular	10^0	0.913	1.025	1.255
Reverse Delta (20^0 Anhedral)	10^0	0.611	0.681	1.834
Delta	10^0	0.637	0.679	0.820
Rectangular	15^0	1.271	1.431	1.760
Reverse Delta (20^0 Anhedral)	15^0	0.836	0.941	2.605
Delta	15^0	0.878	0.991	1.134

Figure 20 shows the plots created in XFLR5 from which the data in Table 4 derives. These plots relate the lift coefficients to angles of attack at respective flight altitudes for the three reference wing configurations tested.

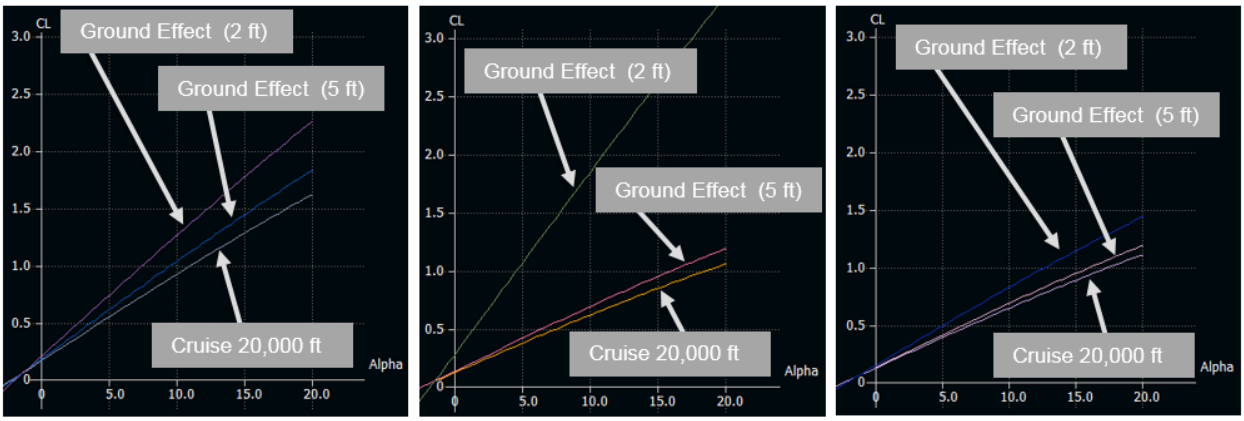

Figure 20: Reference Wing Lift Coefficients at the Three Flight Conditions

In Figure 20, the greatest sloped line in each plot defines the reference wing data for the skim flight condition at an altitude of two feet. The line with the lowest slope magnitude in each plot represents the reference wing data for cruise flight at an altitude of 20,000 feet. The remaining line provides the reference wing data for skim flight conditions at an altitude of five feet. From Figure 20 and Table 4, it was discerned that each reference wing had a different lift coefficient trend. As expected, the Reverse Delta wing with 20□ anhedral, traditionally used for ground-effect vehicles, showed the highest lift coefficients for skim flight at two feet in ground effect, while the Rectangular wing, traditionally used for medium altitude flight, exhibited slightly lower lift coefficients in the same flight condition. Although the Rectangular reference wing did not have the highest lift coefficients in skim at two feet, it did outperform all other reference wings in the cruise flight at 20,000 feet and skim flight at five feet. To help determine if the concepts meet the standard performance required for both mission legs, the Rectangular wing was used as the main reference wing for the performance characteristics comparison of the wing configuration concepts.

3.3 Wing Configuration Concepts

Four wing configuration concepts were analyzed for their ability to perform optimally in both medium-altitude flight and ground-effect flight. These wing configuration concepts utilized the morphing methods of wing sweep and wing anhedral to transform the wings into shapes traditionally used in each flight condition. Wing sweep describes the transition method of rotating the wing in the horizontal plane. Generally, wing sweep is used to improve the aerodynamic efficiency of a wing by delaying shockwaves created on the surface of the wing at higher flight velocities. However, in this case, wing sweep will be utilized to vary the aspect ratio of the wing seen by the free stream airflow. Hypothetically, by rotating the leading edge of the wing 90°, the wing will be capable of achieving both the high aspect ratios preferable for medium-altitude flight and the low aspect ratios preferable for low-altitude flight. Wing anhedral describes the transition method of canting the wingtips downwards perpendicular to the horizontal plane. Conventionally, wing anhedral is used to reduce the stability of an aircraft, making it more maneuverable. However, wing anhedral is also used on the wings of ground-effect vehicles to create a trapped cushion of pressure beneath the wing, further increasing the lift and reducing the drag of the wing. The investigated concepts included a variable sweeping Rectangular wing, a variable anhedral Reverse Delta wing, a variable anhedral Delta wing, and a variable anhedral Rectangular wing. Figure 21 displays the four wing configuration concepts that were analyzed.

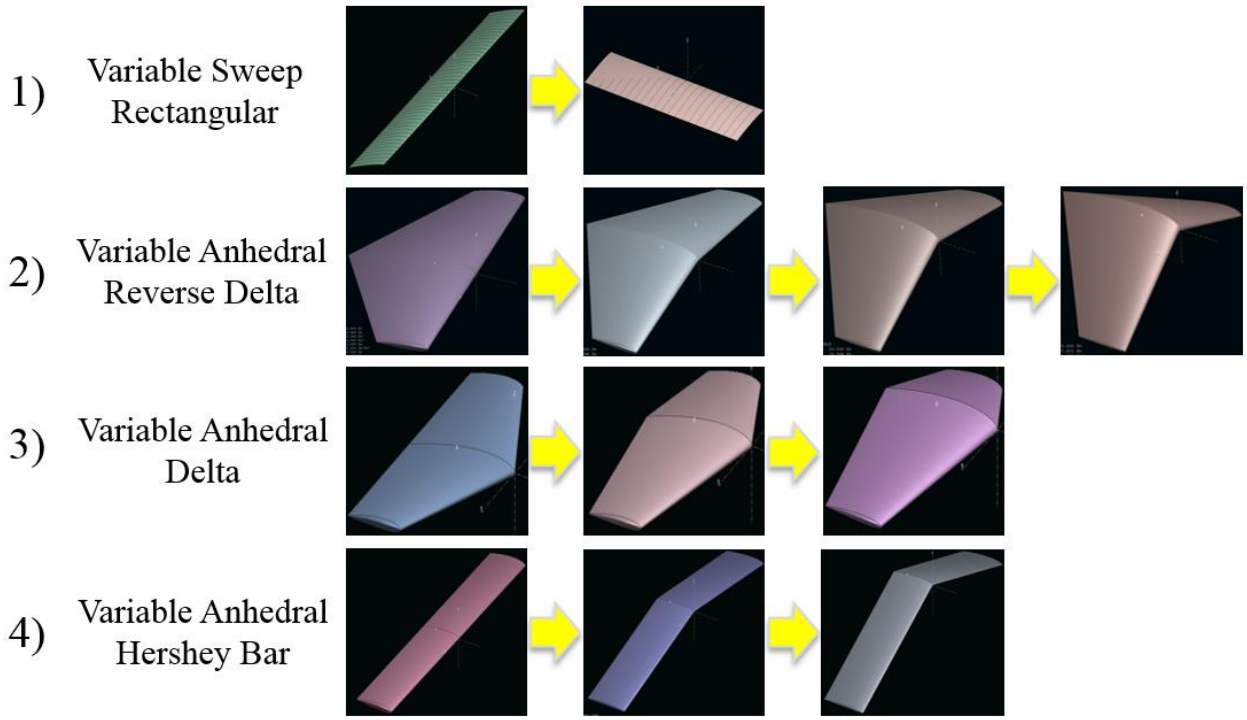

Figure 21: Wing Configuration Concepts Analyzed

3.4 Concept 1: Variable Sweep Rectangular Wing Configuration

With the tools, test parameters, and reference wings established, the wing configuration concepts could begin to be analyzed for the potential of optimum performance characteristics in both medium altitude cruise flight and ground effect skim flight.

The first wing configuration concept analyzed was the variable sweeping Rectangular wing. This method employed the act of sweeping the wing 90° to transition from cruise flight to skim flight. This maneuver enabled the vehicle to transition from a high aspect ratio wing to a low aspect ratio wing. To reiterate, ground effect wings are naturally designed to have a low aspect ratio while medium to high altitude wings are generally designed to have a high aspect ratio. This aspect ratio discrepancy proves to be a challenge when designing a wing to perform optimally in both types of flight conditions. For that reason, the variable sweeping Rectangular wing was investigated for the potential ability to offer

optimum performance characteristics in both cruise flight and skim flight. While analyzing this variable sweep transition method at the same lift conditions, it was notable that the wing-loading in skim proved to be about half the value of the wing-loading in cruise. Additionally, the thrust to weight ratio in skim proved to be roughly three times greater than the thrust to weight ratio in cruise. Figure 22 offers a top view of the variable sweep transition method and provides the relationship between the change in the aspect ratio value when transitioned from cruise to skim.

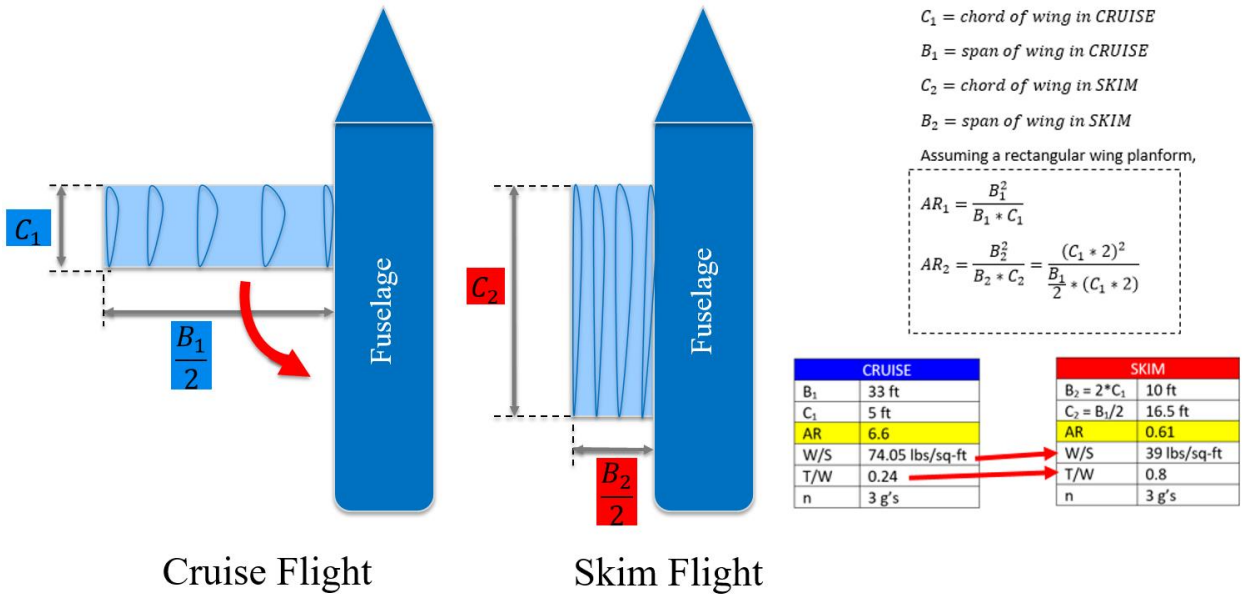

Figure 22: Aspect Ratio Change for Variable Sweep Rectangular Concept

The data shows that ideally, the structure should minimally be designed to handle a wing-loading equal to the wing-loading experienced in cruise and should minimally be capable of attaining a thrust to weight ratio equal to that experienced in skim.

The goal for the variable sweep Rectangular wing concept was to build a wing that had an airfoil in two directions, so that when swept 90° from cruise flight to skim flight, the incoming airflow would interact with another airfoil to produce lift. Figure 23 depicts the desired result.

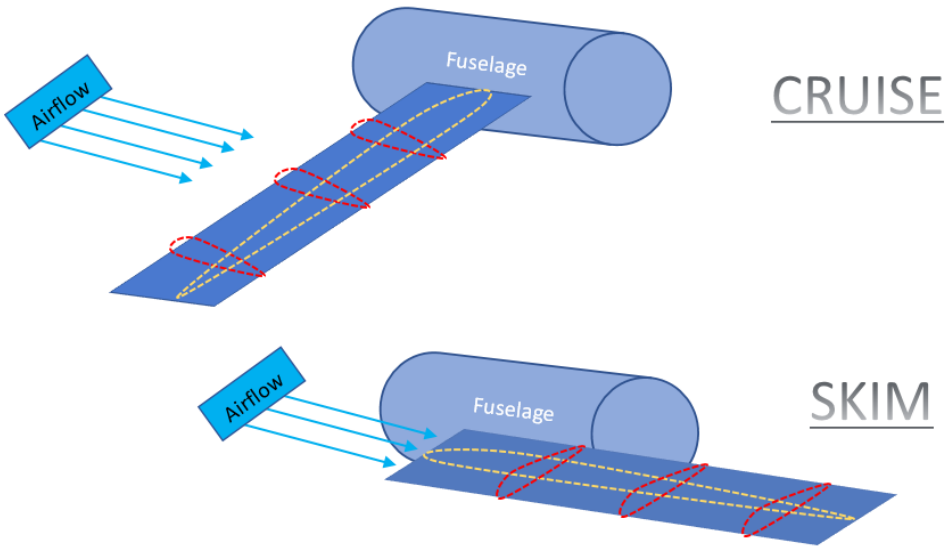

Figure 23: Concept 1 - Variable Sweep Rectangular

To build this wing concept, varying sizes of airfoils had to be stitched together along one axis in order to create the desired airfoil shape for the other axis. This process was mathematically organized so that the stitched together airfoils resulted in creating a preselected airfoil. However, a challenge was encountered during this process. The overall thickness of the wing is determined based upon which flight condition the wing is designed in. To explain, the thickness of an airfoil is defined as a percentage of the overall chord of the airfoil. If the wing were designed in the high aspect ratio cruise flight condition, then the overall thickness of the wing would be thinner because the relative chord of the wing is short. Now, if the wing were swept 90□ and designed in the low aspect ratio skim flight condition, the relative chord of the wing would now be the length of the span of the cruise flight wing. This longer relative chord would make the wing significantly thicker. Therefore, the condition in which the wing is built will determine the overall thickness of the wing. Wing thickness is important because it affects lift, flow separation, achievable aircraft velocities, drag, and other performance characteristics. To analyze this, each thickness variation of the wing was built and run through flow simulations in XFLR5. For ease of reference, the wing designed from the cruise condition position will be termed "Cruise-Built" wing and the wing designed from the skim condition position will be termed "Skim-Built" wing. Figure 24 provides an image of the

Cruise-Built wing in cruise flight, while Figure 25 provides an image of half of the same Cruise-Built wing in skim flight.

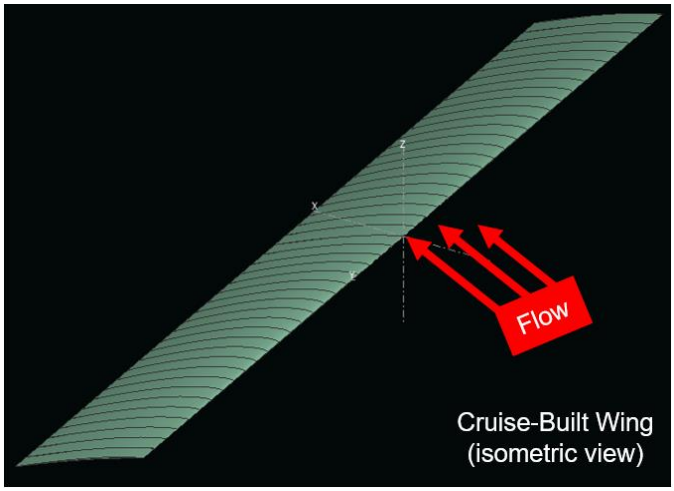

Figure 24: Full Cruise-Built Wing in Cruise (Variable Sweep Rectangular Concept)

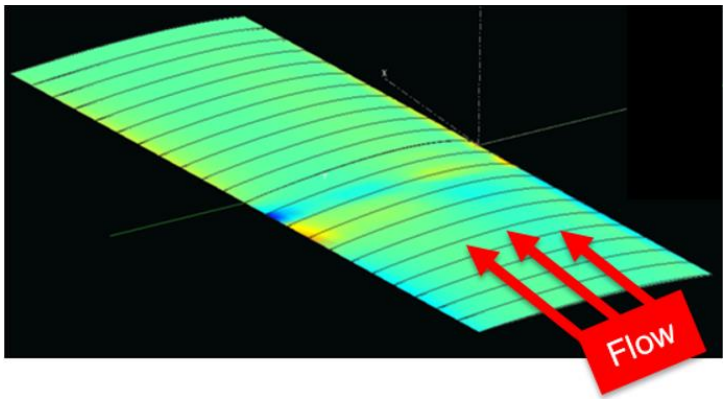

Figure 25: Half of Cruise-Built Wing in Skim (Variable Sweep Rectangular Concept)

Figure 26 and Figure 27 show the Skim-Built wing in cruise flight, while Figure 28 and Figure 29 show the Skim-Built wing in skim flight. The reason there are two figures for the Skim-Built wing in skim flight is because there was a desire to see if only half of the wing rather than the whole wing would significantly change the lift coefficient plot. Figure 28 displays the full Skim-Built wing in skim flight and Figure 29 displays half of the Skim-Built wing in skim flight.

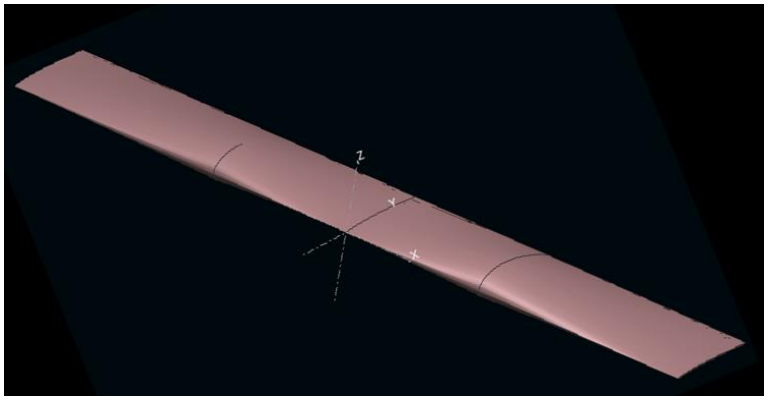

Figure 26: Isometric View of Full Skim-Built Wing in Cruise (Variable Sweep Rectangular Concept)

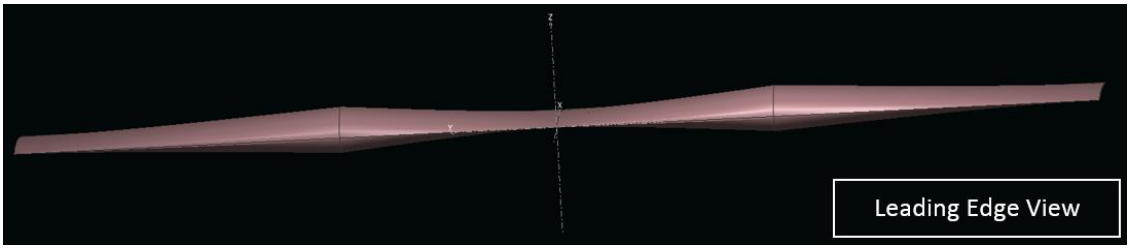

Figure 27: Leading-Edge View of Full Skim-Built Wing in Cruise (Variable Sweep Rectangular Concept)

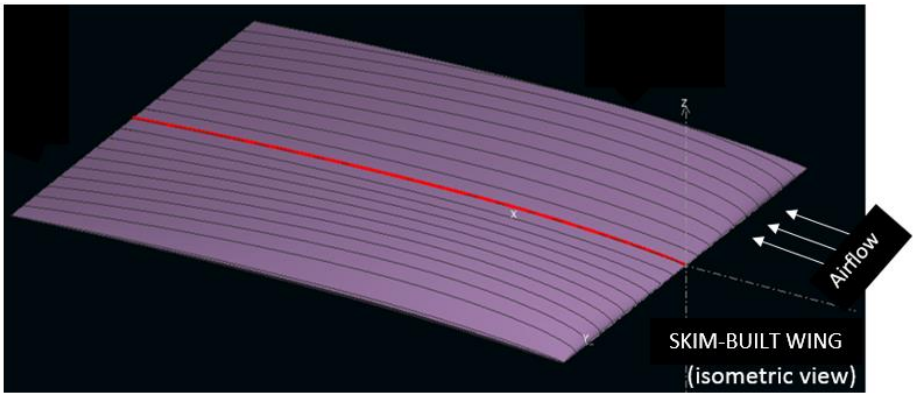

Figure 28: Full Skim-Built Wing in Skim (Variable Sweep Rectangular Concept)

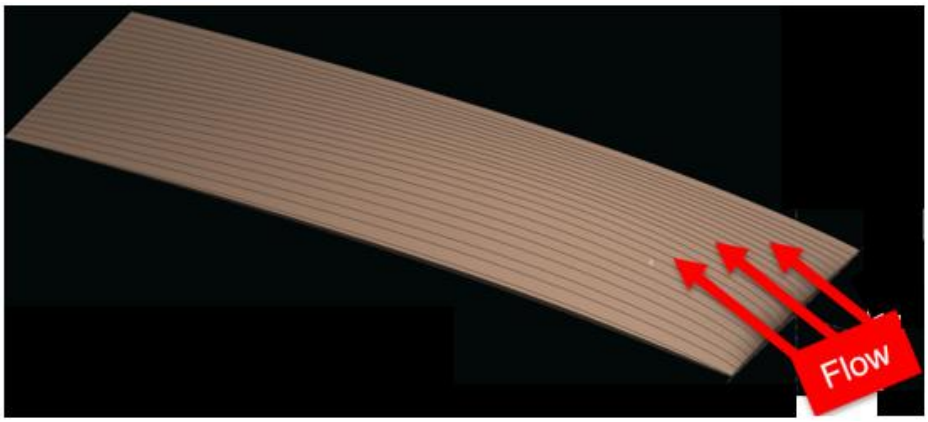

Figure 29: Half of Skim-Built Wing in Skim (Variable Sweep Rectangular Concept)

The Cruise-Built wing and Skim-Built wing were compared to the Rectangular reference wing for their performance characteristic adequacy in each flight mode. To reiterate, the Rectangular wing was established as being capable of the desired performance characteristics for flight at both low and medium altitudes. For cruise flight at an altitude of 20,000 feet, the lift coefficient data sets for the Cruise-Built wing and the Rectangular reference wing are shown in Figure 30.

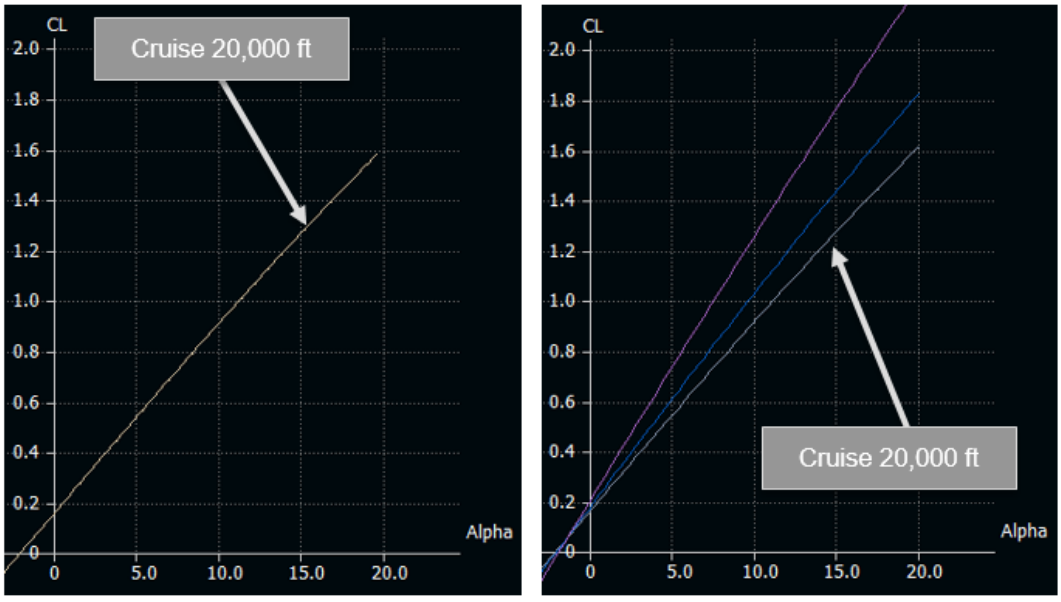

Figure 30: Comparison of Full Cruise-Built Wing (LEFT) and Rectangular Reference Wing (RIGHT) in Cruise

The lift coefficient data sets for the Skim-Built wing and the Rectangular reference wing in cruise flight at 20,000 feet are shown below in Figure 31.

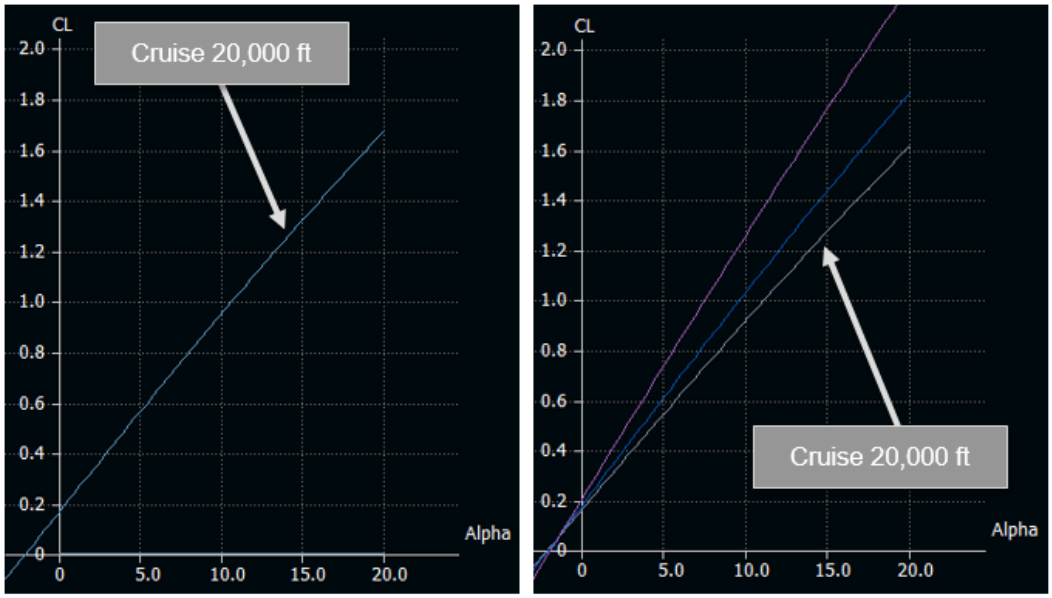

Figure 31: Comparison of Full Skim-Built Wing (LEFT) and Rectangular Reference Wing (RIGHT) in Cruise

From these plots, it was evident that both the Cruise-Built wing and Skim-Built wing perform similarly to the Rectangular reference wing in cruise flight. Since the wing concepts satisfy the cruise flight condition performance requirements for the mission, the performance of the wings in ground effect flight was the next factor examined. For skim flight, the Cruise-Built wing was analyzed in ground effect flight at five feet and the Skim-Built wings were analyzed in ground effect flight at both five feet and two feet. Figure 32 provides the lift coefficient data for half of the Cruise-Built wing in skim flight at a ground effect height of five feet.

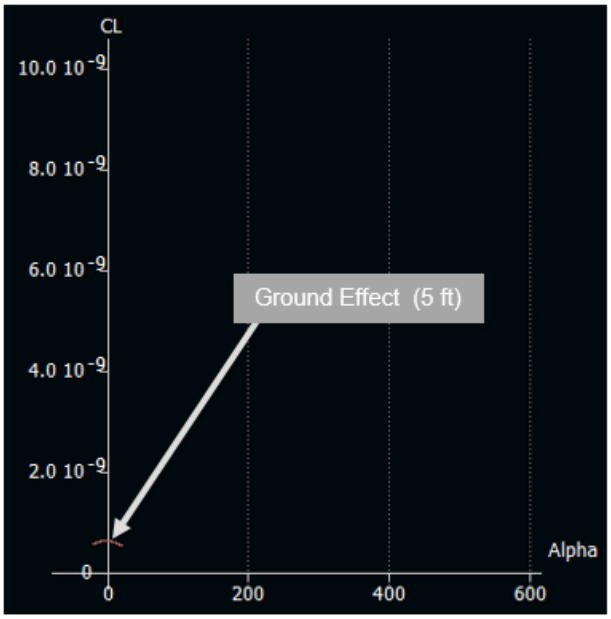

Figure 32: Lift Curve Slope for Half of the Cruise-Built Wing in Skim at Five Foot Ground Effect Height

As shown in the graph, the half Cruise-Built wing in skim flight was not tested at a two foot altitude because the five foot altitude simulation resulted in very low lift coefficient values on the order of 10^{-9}. These performance values were far from sufficient from meeting the performance requirements in comparison to the Rectangular reference wing in the same ground-effect flight conditions. Therefore, this Cruise-Built method of designing the wing in the cruise condition for this wing configuration concept was not viable.

Figure 33 shows the lift coefficient data for the full Skim-Built wing in skim flight positioned adjacently to the lift coefficient data for the Rectangular reference wing in the same skim flight conditions.

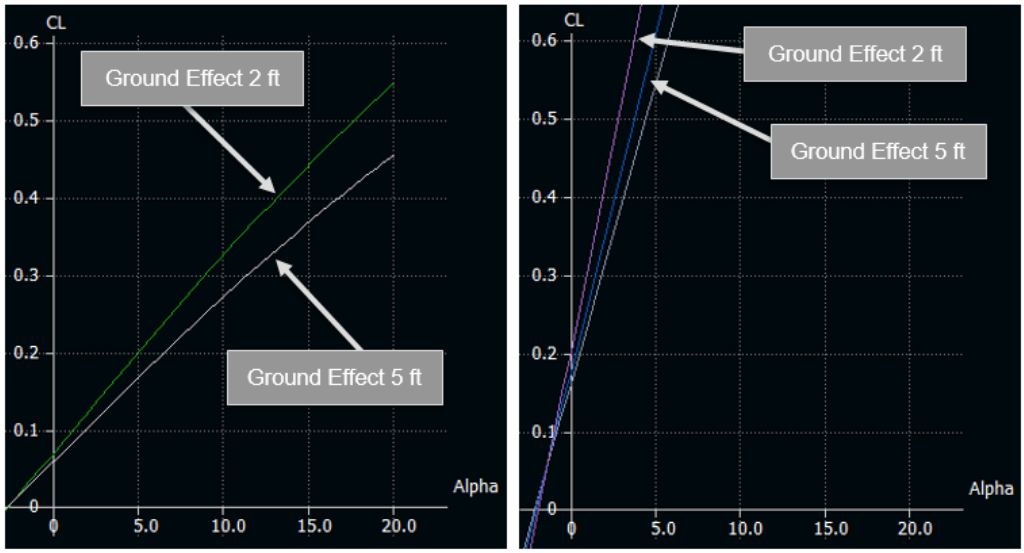

Figure 33: Comparison of Full Skim-Built Wing (LEFT) and Rectangular Reference Wing (RIGHT) in Skim

The Rectangular reference wing outperforms the Skim-Built wing in skim flight. Figure 34 shows the lift coefficient data for half of the Skim-Built wing in skim flight positioned adjacently to the lift coefficient data for the Rectangular reference wing in skim flight.

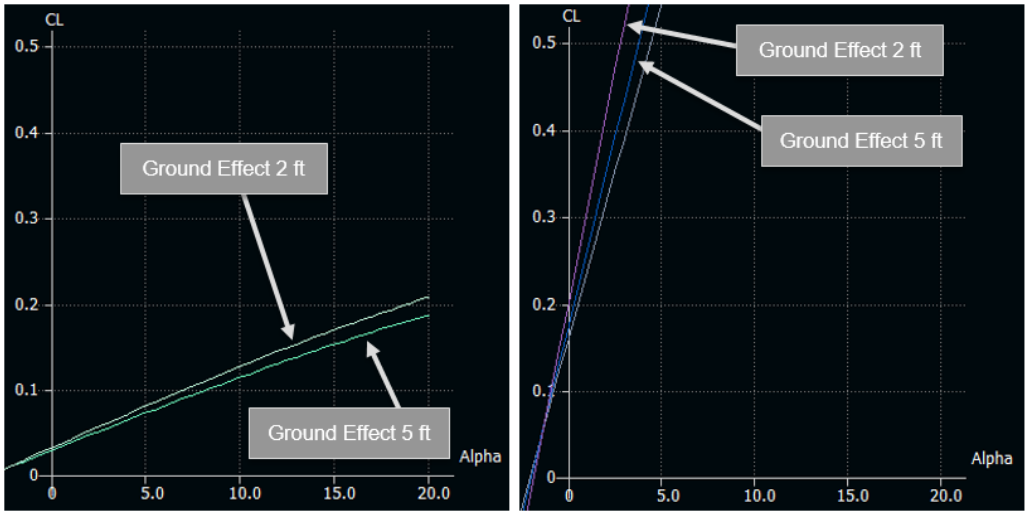

Figure 34: Comparison of Half of the Skim-Built Wing (LEFT) and Rectangular Reference Wing (RIGHT) in Skim

The half Skim-Built wing achieved about half of the performance of the full Skim-Built wing.

To summarize, the variable sweep Rectangular wing configuration concept does function to achieve both high and low aspect ratios for cruise and skim conditions. However, due to the lower lift

coefficients achieved for the concepts as compared to the Rectangular reference wing, neither the Cruise-Built wing nor the Skim-Built wing are viable options for optimizing performance capabilities in these flight conditions. Since the configuration concept was outperformed by the Rectangular reference wing in skim flight, the concept was not compared to the Reverse Delta reference wing, as it outperforms the Rectangular reference wing.

3.5 Concept 2: Variable Anhedral Reverse Delta Wing Configuration

The second wing configuration concept analyzed for optimum performance characteristics in both medium altitude cruise flight and ground effect skim flight was the variable anhedral Reverse Delta wing. Similar to the wings traditionally used on ground effect vehicles, this concept utilized anhedral and the reverse delta shape to achieve enhanced flight characteristics. This concept was based off of the hypothesis that by increasing the angle of wing anhedral of the vehicle as the flight altitude was reduced, improved performance characteristics would be achieved in skim. Then if the vehicle reduced its angle of wing anhedral as it increased in flight altitude, it would experience the performance characteristics of a more traditional wing in cruise. Figure 35 exhibits the increase of wing anhedral for this configuration concept as the vehicle transitions from cruise to skim flight.

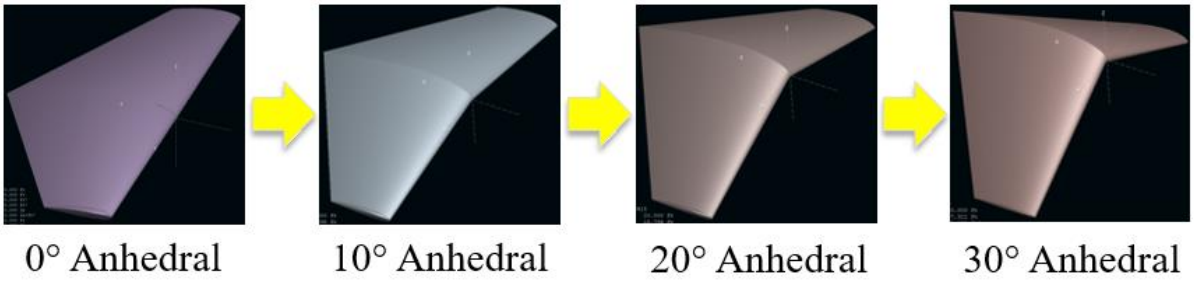

Figure 35: Transition of Concept 2 - Variable Anhedral Reverse Delta Wing from Cruise to Skim

In order to get a picture of the general performance of the wing concept at each degree of anhedral, the wing concept was analyzed in XFLR5 at 0°, 10°, 20°, and 30° angles of anhedral. The

performance of each wing concept at the individual angles of anhedral was compared to the performance of the Rectangular reference wing in both the cruise and skim flight conditions. Figure 36 shows the lift coefficient versus free stream velocity plot for the Reverse Delta wing concept with 0° anhedral. The wing was analyzed in cruise flight at 20,000 feet, skim flight in ground effect at five feet, and skim flight in ground effect at two feet and compared to the lift coefficient data for the Rectangular reference wing in the same conditions.

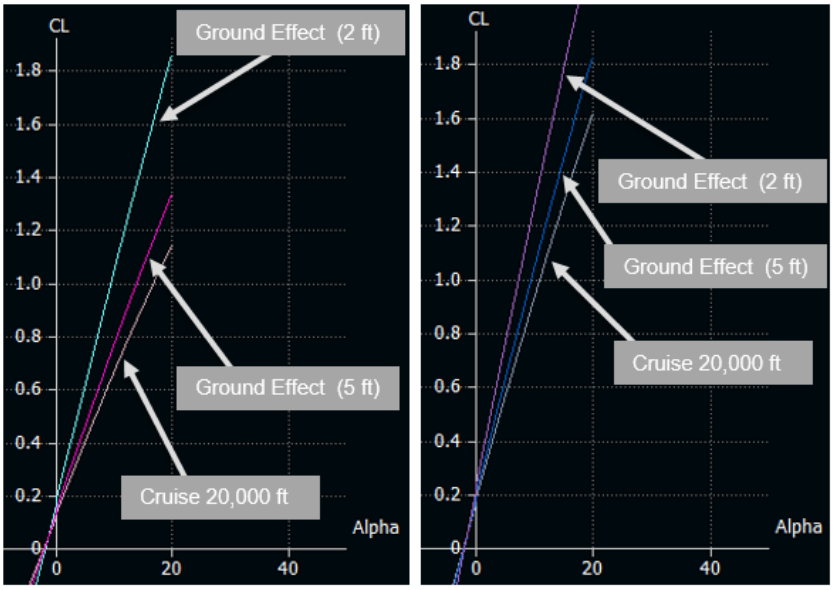

Figure 36: Comparison of Reverse Delta with 0° Anhedral Wing Concept (LEFT) and Rectangular Reference Wing (RIGHT) in Cruise and Skim

The Rectangular reference wing achieves greater lift coefficient slopes than the Reverse Delta wing with 0° anhedral at each flight condition. This highlights that the wing concept at 0° anhedral, where the wing concept should perform optimally in cruise, does not outperform and shows no improvement from the Rectangular reference wing.

Figure 37 shows the comparative lift coefficient data for the configuration concept at 10° anhedral with respect to the Rectangular reference wing.

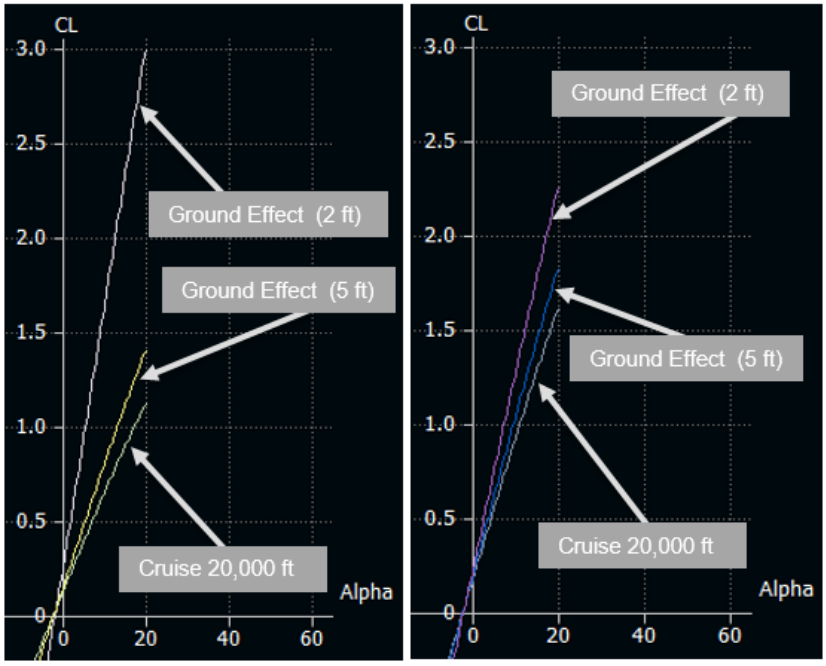

Figure 37: Comparison of Reverse Delta with 10□ Anhedral Wing Concept (LEFT) and Rectangular Reference Wing (RIGHT) in Cruise and Skim

The Rectangular reference wing achieved higher lift coefficients in cruise flight at 20,000 feet and in ground effect skim flight at five feet. However, in ground effect skim flight at two feet, the Reverse Delta wing with 10□ anhedral outperformed the Rectangular reference wing, achieving higher lift coefficients. This confirmed the hypothesis that increased anhedral at low altitudes increases performance characteristics.

Figure 38 shows the comparative lift coefficient data for the configuration concept at 20° anhedral with respect to the Rectangular reference wing.

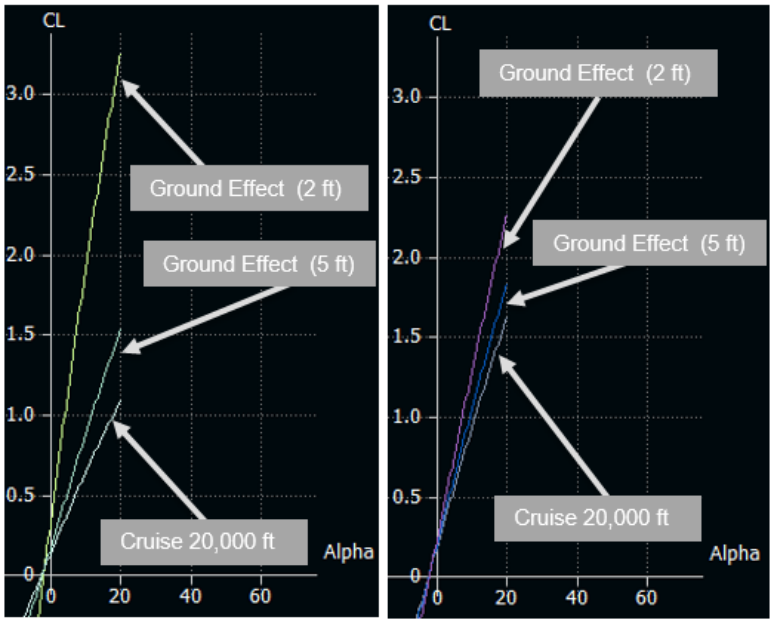

Figure 38: Comparison of Reverse Delta with 20° Anhedral Wing Concept (LEFT) and Rectangular Reference Wing (RIGHT) in Cruise and Skim

The increased anhedral in the wing concept did not increase or decrease the lift coefficients of the Reverse Delta wing concept in cruise. It did however, increase the lift coefficients in ground effect skim flight at both altitudes of five feet and two feet. Although the Reverse Delta wing with 20° anhedral was outperformed by the Rectangular reference wing in cruise, it did show higher lift coefficients in ground effect skim flight at two feet and similar lift coefficients in ground effect flight at five feet. This analysis confirmed that increasing the degree of anhedral of the wing in low altitude ground effect flight increases the flight performance characteristics of the wing.

Figure 39 shows the comparative lift coefficient data for the configuration concept at 30° anhedral with respect to the Rectangular reference wing.

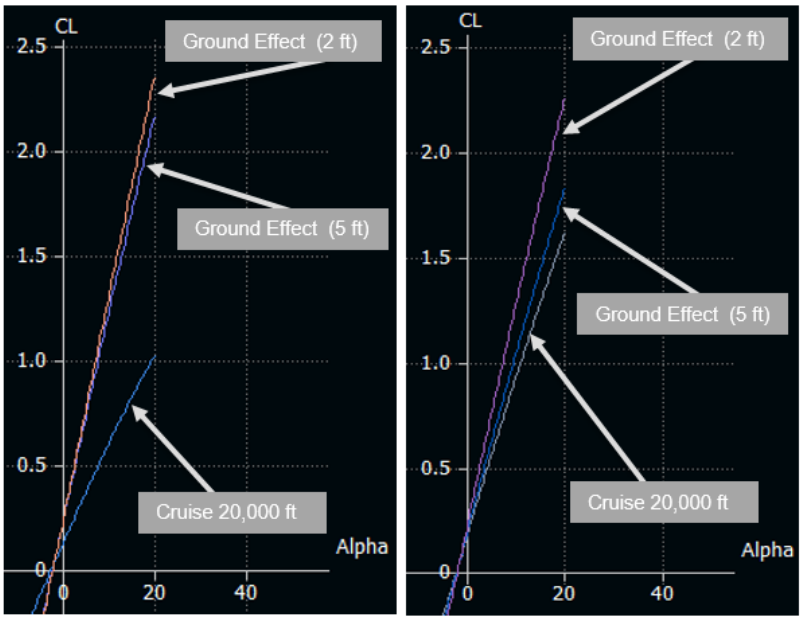

Figure 39: Comparison of Reverse Delta with 30° Anhedral Wing Concept (LEFT) and Rectangular Reference Wing (RIGHT) in Cruise and Skim

The lift coefficients for the Reverse Delta wing with 30° anhedral in the cruise condition decreased due to the increased degree of anhedral. The Rectangular reference wing achieved higher lift coefficients in cruise conditions. In ground effect skim flight at the altitudes of five feet and two feet, the 30° anhedral Reverse Delta wing achieved slightly higher lift coefficients as compared to the Rectangular reference wing.

To summarize the data from the lift coefficient plots, it was determined that no matter the degree of anhedral of the Reverse Delta wing, the Rectangular reference wing achieves much higher lift coefficients in cruise flight conditions. At degrees of anhedral above 30°, the lift coefficients for the Reverse Delta wing in cruise conditions begin to decrease. In ground effect skim flight at altitudes of five feet and two feet, the addition of anhedral on a Reverse Delta wing increases lift coefficient values. However, at degrees of anhedral above 30°, the lift coefficients in ground effect skim flight begin to decrease. Therefore, it was determined that the variable anhedral Reverse Delta wing configuration concept is beneficial in improving the flight performance characteristics in ground effect skim flight, but only at degrees of anhedral around 10° and 20°. Under further investigation, it was determined that the

morphing of the degree of anhedral is not necessary. Since the lift coefficients in cruise flight for the Reverse Delta wing with 10° and 20° anhedral are of similar value to the lift coefficients in cruise flight for the Rectangular reference wing, morphing the wing from 0° to 10° or 20° anhedral is not advantageous. Instead, a Reverse Delta wing with a fixed degree of anhedral around 10° and 20° would prove to have better performance characteristics.

3.6 Concept 3: Variable Anhedral Delta Wing Configuration

The third wing configuration concept investigated for the potential of optimum performance in both cruise flight and skim flight conditions was the variable anhedral Delta wing. Similar to the second wing configuration concept, the variable anhedral Delta wing concept employed the method of varying the anhedral of the wing. The hypothesis behind this concept was that the leading edge sweep and delta planform would enable the wing to perform optimally in high speed cruise flight. The variable anhedral was projected to improve the skim flight characteristics of the wing by reducing the wing tip vortices and creating a trapped high-pressure region beneath the wing. Figure 40 exhibits the increasing degree of anhedral during the transition of this concept from cruise flight to skim flight.

Figure 40: Transition of Concept 3 - Variable Anhedral Delta Wing from Cruise to Skim

To reduce computational time, the third wing configuration concept was analyzed at anhedral degrees of 0°, 10°, and 20° only. For, the XFLR5 lift coefficient data. To evaluate the viability of the wing configuration concept to combine medium altitude flight and skim flight characteristics, the XFLR5 lift

coefficient data of each anhedral degree variation of the wing concept was compared to lift coefficient data of the Rectangular reference wing. Each wing was evaluated in cruise flight at 20,000 feet, skim flight at five feet, and skim flight at two feet.

Figure 41 displays the lift coefficient data for the Delta wing concept at 0° anhedral with respect to the lift coefficient data of the Rectangular reference wing.

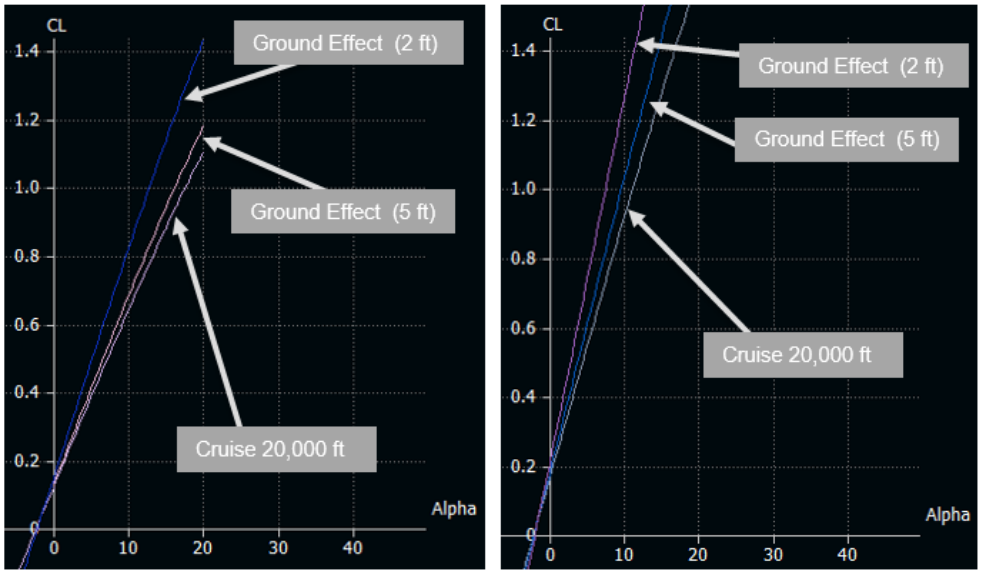

Figure 41: Comparison of Delta with 0° Anhedral Wing Concept (LEFT) and Rectangular Reference Wing (RIGHT) in Cruise and Skim

The plots in Figure 41 show that the Delta wing with 0° anhedral has significantly lower lift coefficients in all flight conditions than the Rectangular reference wing.

Figure 42 presents the lift coefficient data for both the Delta wing with 10° anhedral and the Rectangular reference wing.

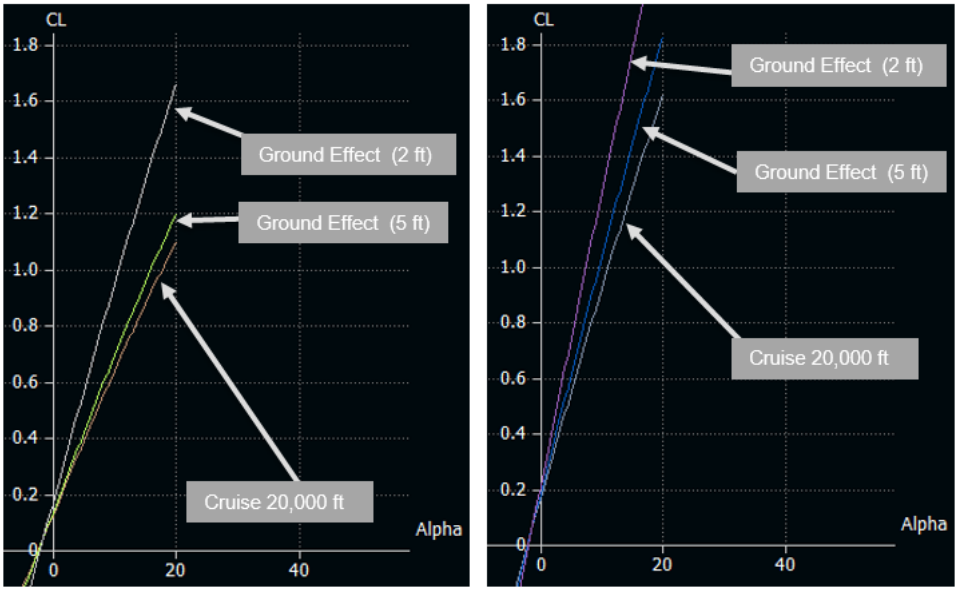

Figure 42: Comparison of Delta with 10□ Anhedral Wing Concept (LEFT) and Rectangular Reference Wing (RIGHT) in Cruise and Skim

The addition of 10° of anhedral did not affect the coefficient of lift in the cruise condition for the Delta wing. However, it did increase the lift coefficient for the Delta wing in the skim flight condition at the altitude of two feet. In all flight conditions, the Rectangular reference wing achieved higher lift coefficients than the Delta wing with 10° anhedral.

Figure 43 shows the lift coefficient data for both the Delta wing with 20° anhedral and the Rectangular reference wing.

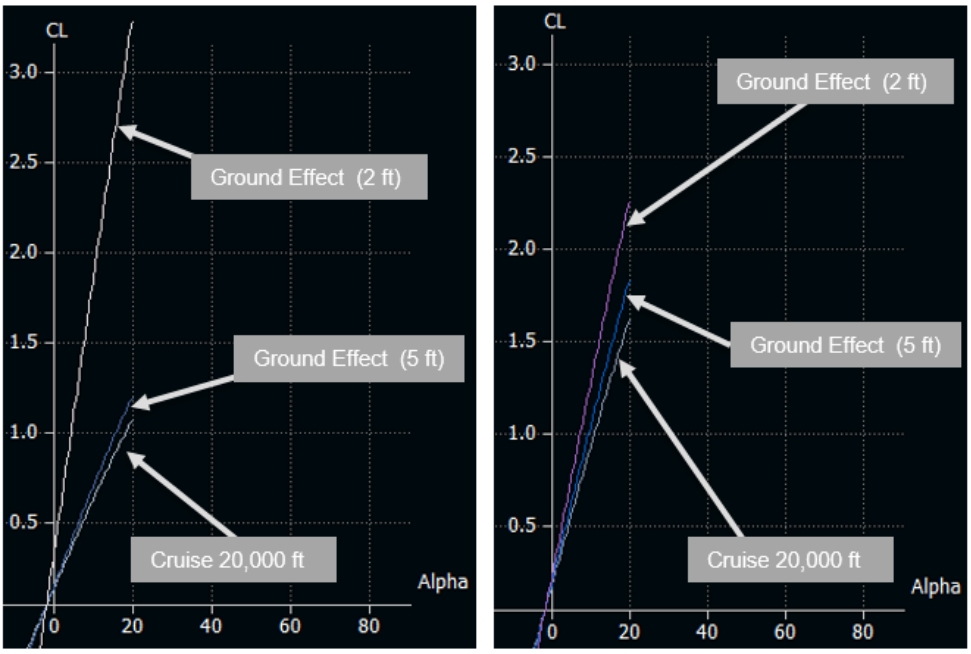

Figure 43: Comparison of Delta with 20□ Anhedral Wing Concept (LEFT) and Rectangular Reference Wing (RIGHT) in Cruise and Skim

The increased degree of anhedral significantly increased the lift coefficients of the Delta wing in the skim flight at the altitude of two feet. However, it did not affect the lift coefficients of the Delta wing in either the cruise flight at 20,000 feet condition or the ground effect skim flight at five feet condition. In this case, the Rectangular reference wing achieved higher coefficients of lift in all flight conditions except for skim flight at the altitude of two feet.

From the lift coefficient data for the third wing configuration concept, it was determined that in cruise flight, the Rectangular reference wing is capable of higher lift coefficients in comparison to the variable anhedral Delta wing concept. In skim, the variable anhedral Delta wing is only capable of higher coefficients of lift in skim flight at very low ground effect heights around two feet. The inconsistent increase of lift coefficients at various ground effect skim heights and the lower lift coefficients achieved in cruise flight render the variable anhedral Delta wing configuration concept implausible for optimally performing in both medium altitude cruise and ground effect skim flight.

3.7 Concept 4: Variable Anhedral Rectangular Wing Configuration

The fourth configuration concept tested for optimum performance in both cruise flight and skim flight was the variable anhedral Rectangular wing. This concept employed the use of changing the degree of anhedral of a rectangular shaped wing. The hypothesis behind this concept was that at 0° anhedral the wing would replicate the performance of a traditional Rectangular wing. As the degree of anhedral increased, the flight performance in skim was projected to improve due the reduction of wing tip vortices. Figure 44 exhibits the increase of anhedral of the wing during the transition from cruise flight to skim flight.

Figure 44: Transition of Concept 4 - Variable Anhedral Rectangular from Cruise to Skim

The variable anhedral Rectangular wing concept was evaluated in XFLR5 at two anhedral deflection degrees, 10° and 20°. Since the Rectangular reference wing models the variable anhedral Rectangular wing concept at 0° anhedral, the wing concept was not evaluated at 0° anhedral. Each wing was tested in cruise flight at 20,000 feet, skim flight in ground effect at five feet, and skim flight in ground effect at two feet. The lift coefficient results were then compared to those of the Rectangular reference wing. Figure 45 shows the lift coefficient data for the Rectangular wing concept with 10° anhedral and the Rectangular reference wing.

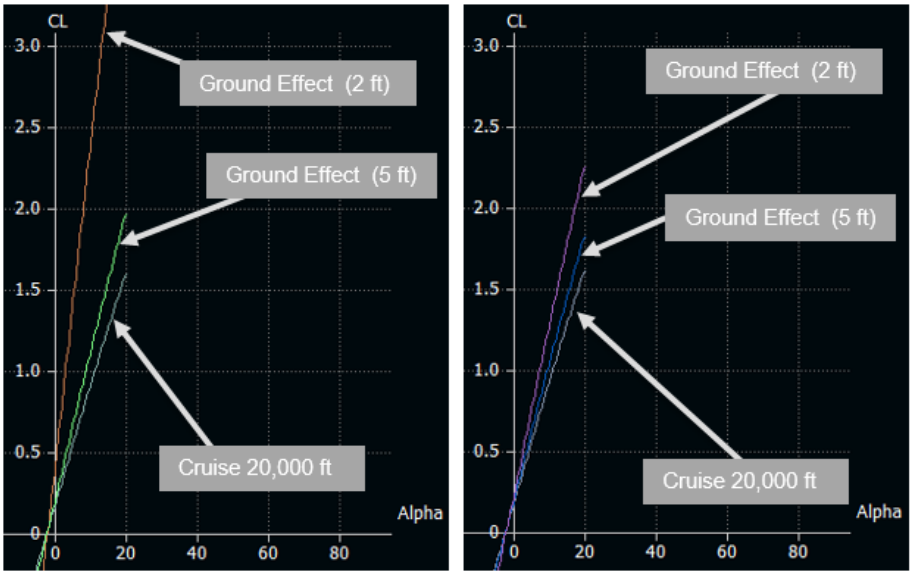

Figure 45: Comparison of Rectangular with 10° Anhedral Wing Concept (LEFT) and Rectangular Reference Wing (RIGHT) in Cruise and Skim

The introduction of anhedral to the Rectangular wing significantly increased the lift coefficients achievable in skim flight at an altitude of two feet. The lift coefficients for the Rectangular wing concept with 10° anhedral in cruise flight and skim flight at five feet were unaffected by the anhedral. Therefore, the addition of anhedral to the Rectangular wing is beneficial to achieving optimum performance in skim flight.

Figure 46 displays the lift coefficient data for both the Rectangular wing concept with 20° anhedral and the Rectangular reference wing.

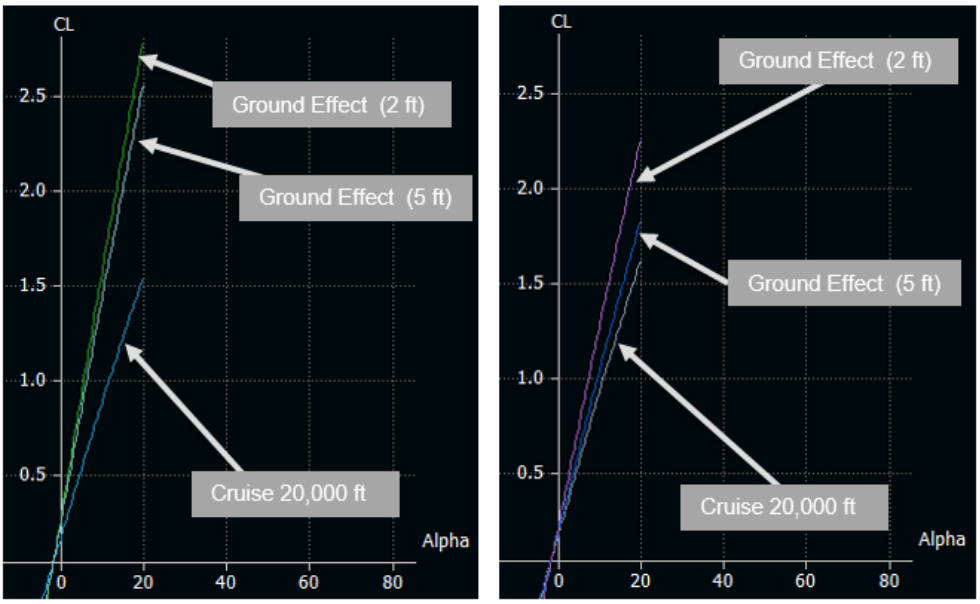

Figure 46: Comparison of Rectangular with 20° Anhedral Wing Concept (LEFT) and Rectangular Reference Wing (RIGHT) in Cruise and Skim

The increased anhedral slightly reduced the magnitude of the lift coefficients in cruise. However, in skim flight at both altitudes of five feet and two feet, the lift coefficient values were significantly increased.

From this data, it was evident that in cruise, the anhedral slightly reduced the achievable lift coefficients of the concept wing. Conversely, in skim, the anhedral increased the lift coefficients of the concept wing. Interestingly, in skim flight at an altitude of two feet, the lift coefficient slope of the Rectangular wing concept with 10° of anhedral experienced a significant increase in magnitude, while the lift coefficient slope for the Rectangular wing concept with 20° anhedral in the same flight condition only saw a slight increase. The discrepancy for the variable anhedral Rectangular wing is that at higher degrees of anhedral, the magnitude of lift coefficient values are less spread out between skim flight altitudes. For example, the lift coefficient slopes for the Rectangular wing with 20° anhedral in Figure 46 for ground effect flight at two feet and ground effect flight at five feet are close in magnitude. However, the lift coefficient slopes for the Rectangular wing with 10° anhedral in Figure 45 at the same two ground effect heights are very different in magnitude. The large lift coefficient slope differential between the two small

skim heights offers unsteady flight characteristics should the skim height change slightly during operation.

Since the lift coefficients of the wing concept in the cruise flight condition did not change considerably when anhedral was added, it was determined that employing variable anhedral to a Rectangular style wing is unnecessary. However, the data did show that there was a benefit to creating a fixed wing version of the Rectangular wing with a large degree of anhedral. This degree of anhedral had to be larger in magnitude since the lower degrees, like that of 10°, proved to have inconsistent lift coefficient increases as the skim flight altitude was decreased.

3.8 Selecting the Ideal Wing Configuration

From the wing configuration concepts analyzed, three configurations were identified as the most capable of performing optimally in both cruise and skim flight conditions. The benefits of morphing the wings proved too minimal to outweigh the added weight penalties, mechanical complexities, and control challenges associated with implementing the transforming concepts. In spite of the minimal results for the morphing wing configuration concepts, a few fixed wing configurations with anhedral showed great potential for optimum performance characteristics in both cruise and skim flight. Figure 47 displays the three fixed wing configuration concepts identified as potential candidates.

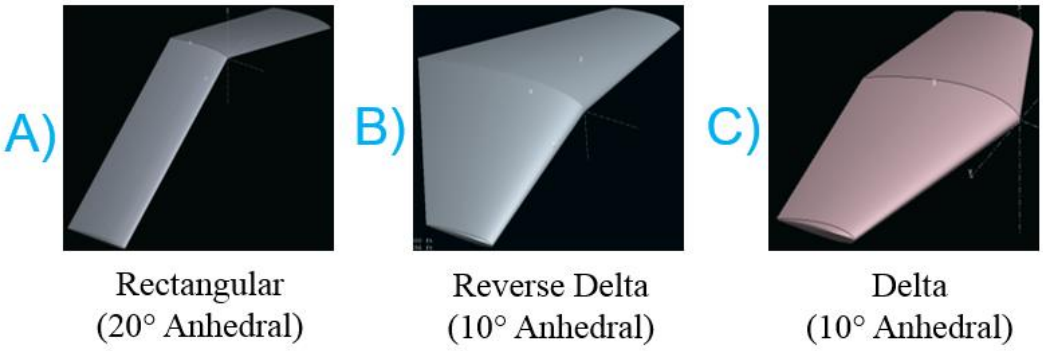

Figure 47: Final Fixed Wing Configuration Concepts

To determine which of the three configuration concepts most optimally combined the performance characteristics of medium altitude cruise flight and ground effect skim flight, the plots from Figure 16 and Figure 17 were referred to again. The foundational idea obtained from these plots was that in order to achieve all of the desired performance requirements for the SUAV, a very low lift coefficient at 0° angle of attack and a relatively high lift coefficient around 12° to 20° angle of attack had to be achievable by the selected wing configuration in both the cruise flight and skim flight conditions. Additionally, the moment coefficients of the wing in both flight conditions had to be of a reasonable magnitude, as it would affect the size of the tail and the overall drag of the vehicle. To exemplify the process for determining the performance characteristics of the three wings, the data from the analysis of the Reverse Delta with 10□ anhedral is shown below. Figure 48 shows the lift coefficient data of the wing, highlighting the low lift coefficient values achievable at small angles of attack and the higher lift coefficient values achievable at larger angles of attack.

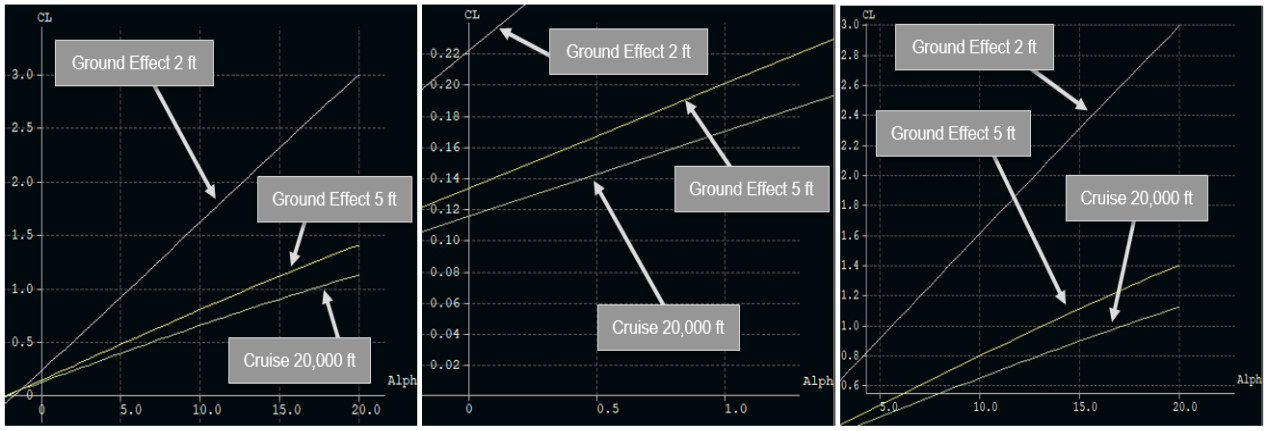

Figure 48: Lift Curve Slopes for the Reverse Delta with 10° Anhedral in All Flight Conditions

By relating the lift coefficient values in Figure 48 to the lift coefficient versus flight velocity plots of Figure 16 and Figure 17 that were created earlier in the study, an idea of the performance capabilities of the Reverse Delta with 10° anhedral were determined. Figure 49 shows how the lift coefficient data of the Reverse Delta with 10° anhedral correlates to the lift coefficient versus velocity plot from Figure 16 to determine the maximum speed and minimum loiter speed achievable in cruise flight.

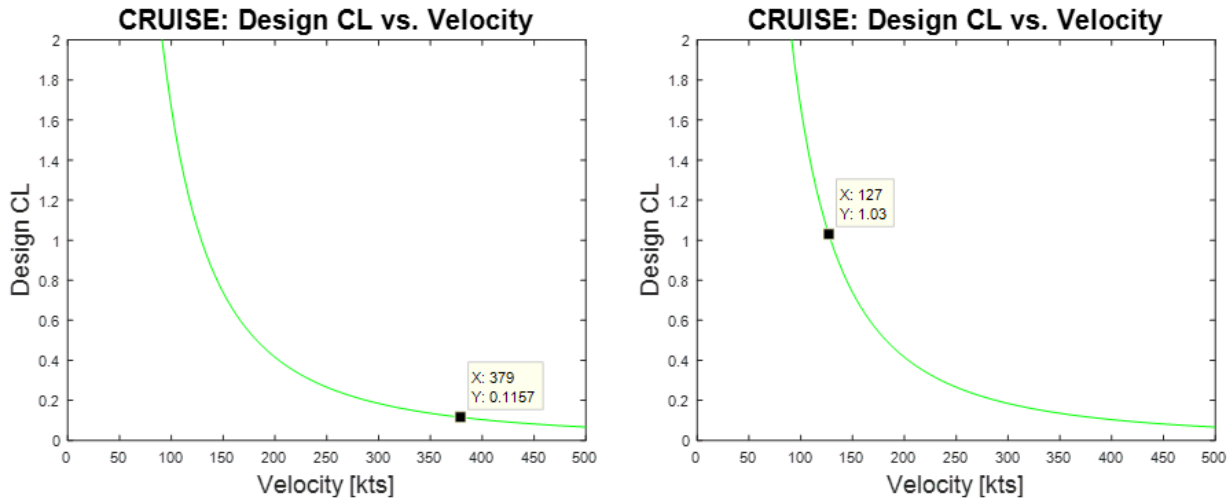

Figure 49: Maximum Cruise Speed (LEFT) and Minimum Loiter Speed (RIGHT) for Reverse Delta with 10° Anhedral Fixed Wing Concept

With a minimum lift coefficient of 0.1157 at 0° angle of attack in cruise conditions, the Reverse Delta wing with 10° anhedral achieved a maximum cruise speed of 379 knots (436 mph), which met the minimum desired performance characteristic of a 333 knot cruise speed. The maximum lift coefficient of 1.03 for the wing at 18° angle of attack in cruise conditions achieved a reasonably low loiter speed of 127 knots (146 mph).

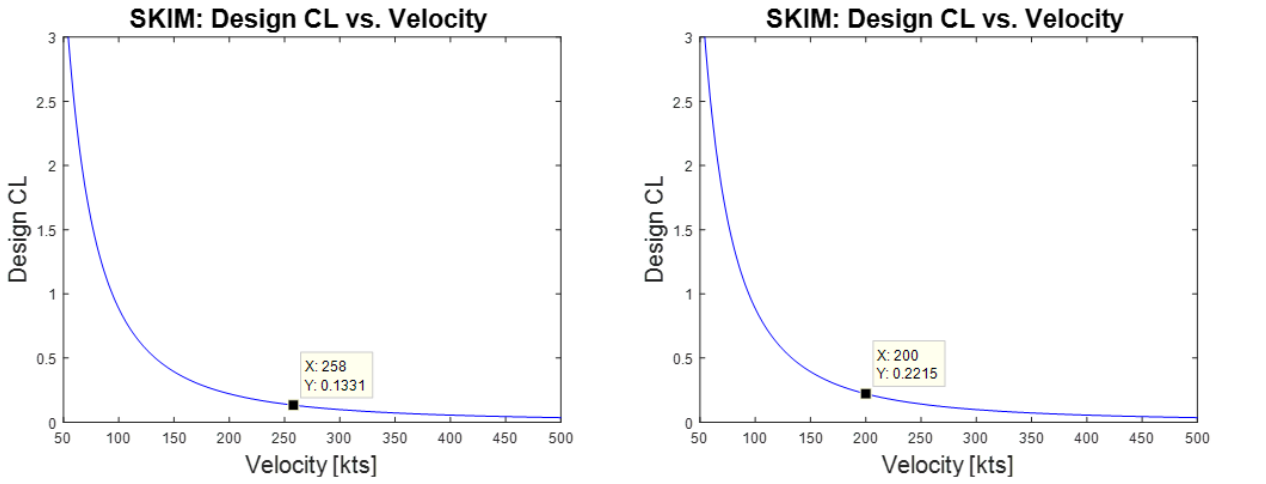

Max Skim Speed @ 5 feet = 258 knots (297 mph) Max Skim Speed @ 2 feet = 200 knots (230 mph)

Figure 50: Maximum Skim Speed at Five Feet Ground Effect Height (LEFT) and at Two Feet Ground Effect Height (RIGHT) for Reverse Delta with 10□ Anhedral Fixed Wing Concept

With a lift coefficient of 0.1331 at 0° angle of attack in the skim at an altitude of five feet flight condition, the Reverse Delta wing with 10° anhedral achieved a maximum skim speed of 258 knots, which satisfied the high skim speed desired performance requirement. Similarly, the wing still achieved a relatively high skim speed of 200 knots with a lift coefficient of 0.2215 at 0° angle of attack.

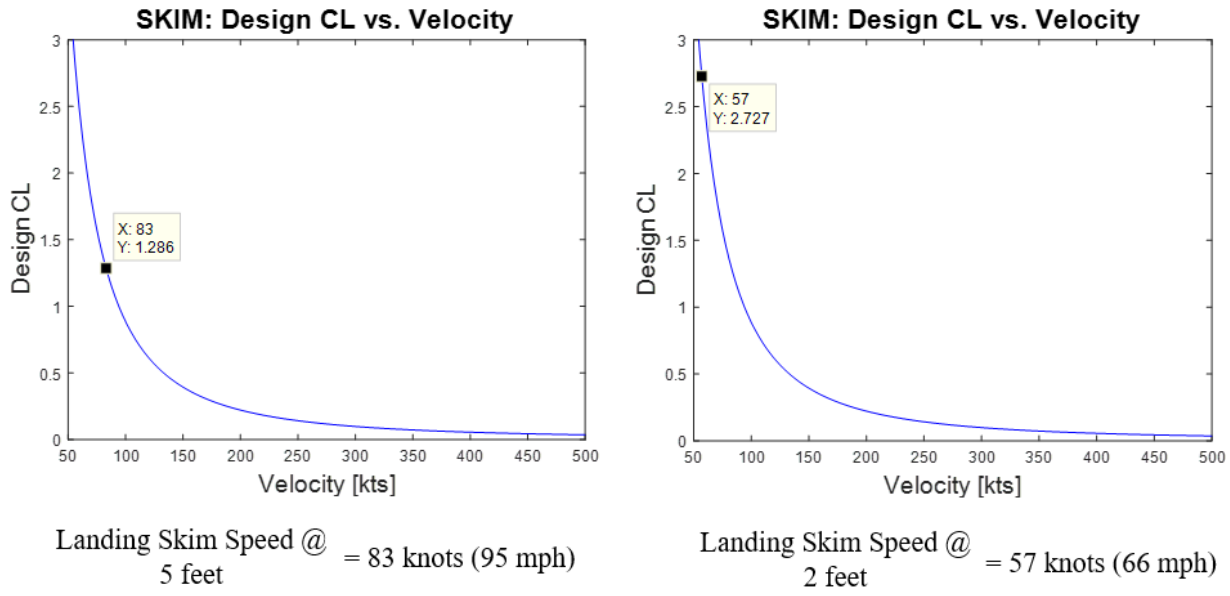

Figure 51: Landing Speed in Skim at Five Foot Ground Effect Height (LEFT) and at Two Foot Ground Effect Height (RIGHT) for Reverse Delta with 10° Anhedral Fixed Wing Concept

In skim flight conditions at an altitude of five feet, the Reverse Delta wing with 10° anhedral wing achieved a maximum lift coefficient of 1.29, translating to a landing speed of 83 knots (95 mph). In skim at an altitude of two feet flight condition, the wing achieved a maximum lift coefficient of 2.73 at 18° angle of attack, translating to a landing speed of 57 knots (66 mph). These low landing speeds satisfied the desired performance characteristic for a low landing speed in skim flight.

As these lift coefficients did initially meet the desired performance requirements for the SUAV, each lift coefficient still had to be compared to their respective coefficients of moment. If the moment coefficient associated with the lift coefficient was too large, the lift coefficient at that angle of attack was not a viable option since the size of the stabilizing surfaces required to balance those moments would be too large. Figure 52 shows a plot of the moment coefficients experienced at the various angles of attack in cruise flight at 20,000 feet, skim flight at a ground effect height of five feet, and skim flight at a ground effect height of two feet for the Reverse Delta wing with 10° anhedral concept.

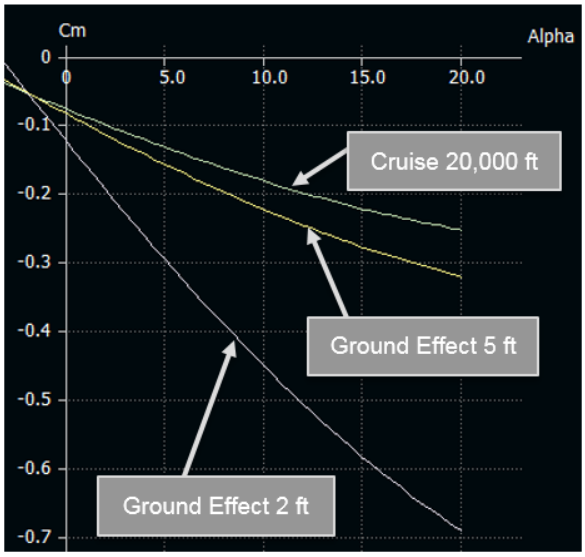

Figure 52: Moment Curve for Reverse Delta with 10□ Anhedral Fixed Wing Concept

Figure 52 shows that the magnitude of the moment coefficient grows significantly for the skim at an altitude of two feet flight condition in comparison to the cruise at 20,000 feet flight condition. This observation highlighted the balancing act of achieving high lift coefficients at reasonable moment coefficient values.

Figure 53 displays the moment coefficient plots for the three final wing configuration concepts.

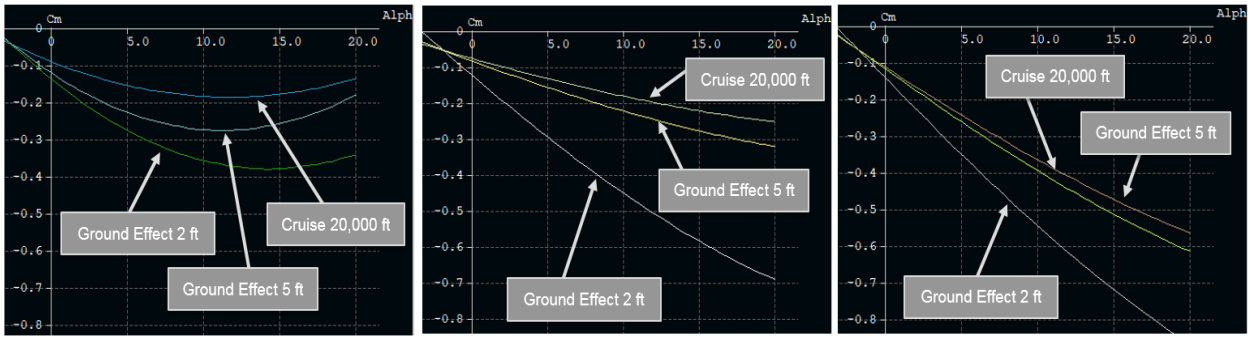

Rectangular (20° Anhedral) | Reverse Delta (10° Anhedral) | Delta (10° Anhedral)

Figure 53: Moment Curves for Fixed Wing Configuration Concepts in All Flight Conditions

Among the three final wing configurations, the Rectangular wing with 20° anhedral configuration had the lowest magnitude of maximum moment coefficient experienced in each flight mode. Notably, among the three wing configurations, it showed the lowest magnitude of moment coefficient in the skim flight

condition at a ground effect altitude of two feet, a flight condition where the largest moments are experienced.

Figure 54 displays the lift coefficient plots for three final wing configurations.

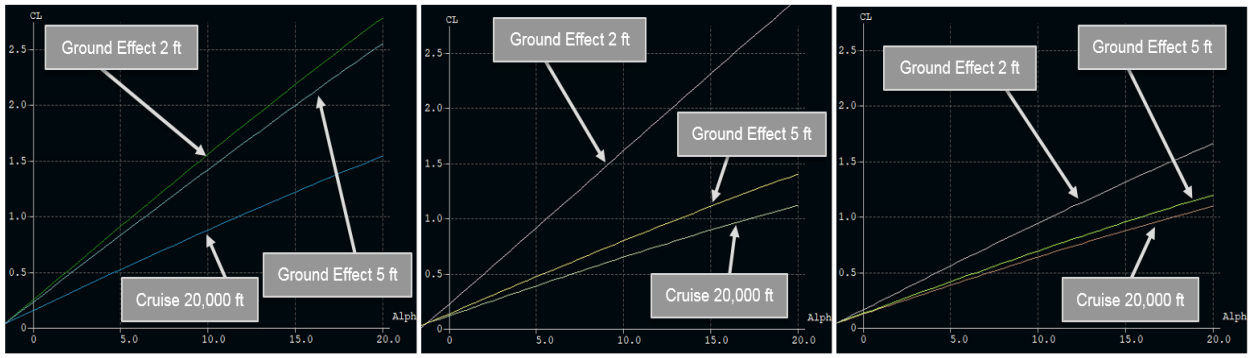

Figure 54: Lift Curve Slopes for Fixed Wing Configuration Concepts in All Flight Conditions

From Figure 54, it was noted that among all of the final wing configurations, the Rectangular wing with 20° anhedral exhibited lift coefficient slopes closest in magnitude for the skim flight at a ground effect height of five feet and the skim flight at a ground effect height of two feet flight conditions. This small differential in lift coefficient slopes for the skim flight modes was important because it showed that the vehicle did not have to be very close to a surface to achieve enhanced lift coefficients and that small changes in ground effect height would not drastically affect the performance of the vehicle.

Figure 55 shows magnified views of the lift coefficient plots for the three final wing configurations from 0° to 1.2° angle of attack. These plots highlighted the lowest achievable lift coefficients for each wing configuration, a factor that directly correlated to the maximum speed the wing could achieve in both cruise and skim flight.

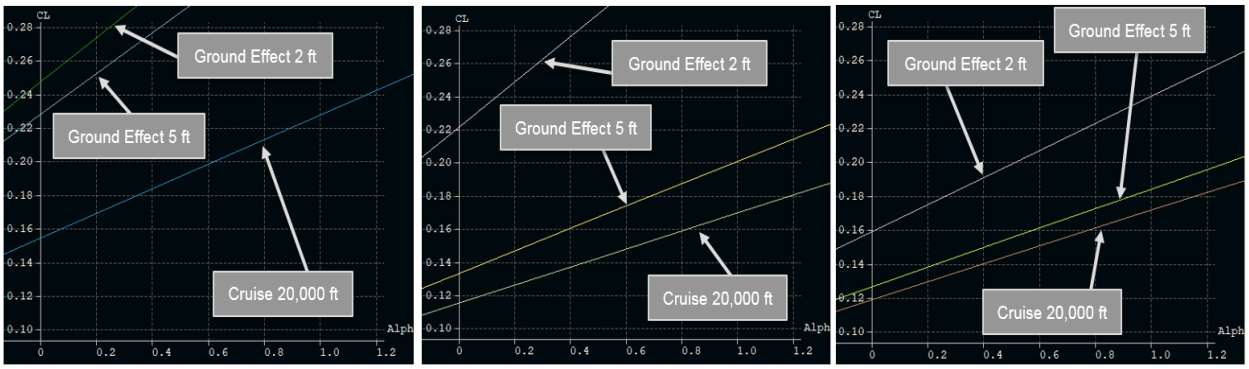

Figure 55: Lift Curve Slopes from 0° to 1.2° Angle of Attack for Fixed Wing Configuration Concepts in All Flight Conditions

Figure 55 showed that the Reverse Delta wing with 10° anhedral achieved the lowest lift coefficients at 0° angle of attack in the cruise flight mode. The Delta wing with 10° anhedral achieved the lowest lift coefficients in the skim flight modes. Lastly, it was noted that the Rectangular wing with 20° anhedral had the highest lift coefficient values among all three of the final wing configuration concepts.

Figure 56 shows magnified views of the lift coefficient plots for the three final wing configurations from 10° to 20° angle of attack. These plots highlighted the highest achievable lift coefficients for each wing configuration, a factor that directly correlated to the minimum landing speed for the wing in skim flight and the minimum loiter speed of the wing in cruise flight.

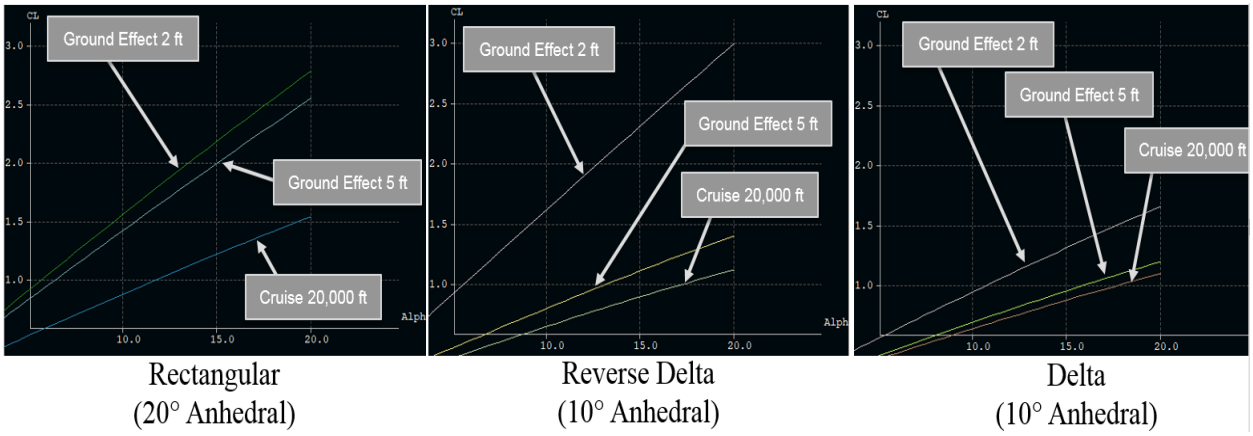

Figure 56: Lift Curve Slope from 10° to 20° Angle of Attack for Fixed Wing Configurations in All Flight Conditions

Figure 56 shows that among all of the final wing configuration concepts, the Rectangular wing with 20° anhedral achieved the highest lift coefficient in cruise flight. Although the Reverse Delta wing with 10° anhedral achieved the highest lift coefficient in skim flight at an altitude of two feet, it was the Rectangular wing the 20° anhedral that achieved the highest lift coefficient in skim flight at an altitude of five feet. Additionally, the lift coefficient of the Rectangular wing with 20° anhedral in skim flight at an altitude of two feet was not far in magnitude from that of the Reverse Delta wing with 10° anhedral. The Delta wing with 10° anhedral significantly underperformed the other two final wing configurations with the lowest lift coefficient values for each flight mode.

By comparing the moment coefficient plots from Figure 53 and the lift coefficient plots from Figure 54, the wing configurations were evaluated for sufficiency in satisfying the desired performance characteristics and the ideal wing configuration concept was determined. The Delta wing with 10° anhedral achieved the lowest overall lift coefficient values among all three final wing configuration concepts. This translated to the highest achievable flight speeds in cruise and skim conditions. However, the Delta wing with 10° anhedral also achieved the lowest maximum lift coefficient values among the three final wing configuration concepts, translating to the highest landing speed values. The Rectangular wing with 20° anhedral achieved the largest lift coefficients at 0° angle of attack, translating to the slowest cruise and skim flight speeds of the three final wing configuration concepts. However, the Rectangular wing with 20° anhedral did show the highest overall maximum lift coefficients for the flight modes, translating to the slowest landing and loiter speeds. The Reverse Delta wing with 10° anhedral showed the second lowest overall lift coefficients at 0° angle of attack, translating to the second fastest cruise and skim flight speeds. It also showed the second highest overall maximum lift coefficients for the flight modes, translating to the second slowest landing and loiter speeds of the three wings. Therefore, with respect to the lift coefficient plots, the Rectangular wing with 20° anhedral and the Reverse Delta

wing with 10° anhedral stood out as the best two candidates for optimizing flight in both the cruise and skim flight scenarios.

Lastly, the coefficient of moment plots for the final three wing configurations in Figure 53 were examined. As mentioned earlier, the Rectangular wing with 20° anhedral maintained the lowest moment coefficient values for all three flight condition scenarios. The Reverse Delta wing with 10° anhedral showed the second lowest magnitude of moment coefficient values. And the Delta wing with 10° anhedral displayed the greatest magnitude of moment coefficient values. High magnitudes of moment coefficients are detrimental because they increase the size of the stabilizing surfaces necessary to balance the aircraft. Moment coefficient values have the greatest impact in ground effect flight since the moment coefficients are magnified by the phenomenon. Therefore, the high magnitude of moment coefficients, rendered the Delta wing with 10° anhedral configuration concept an unviable option.

Reasonable values for high angles of attack range from 10° to 15°. For that reason, the lift coefficient values of the Reverse Delta wing with 10° anhedral were examined in the skim flight conditions to identify if the values at those angles of attack achieved low enough stall speeds for landing. The moment coefficients at those angles of attack were then evaluated for adequacy. At 13° angle of attack in skim flight at an altitude of two feet, the Reverse Delta with 10° anhedral configuration was capable of a 76 mph landing speed with a reasonable moment coefficient magnitude of 0.52. However, with the addition of flow control devices and larger tail surfaces, the wing could be operable at higher angles of attack offering even lower achievable landing speeds around 59 mph. Figure 57 shows the correlation between lift coefficient values and achievable landing speeds in skim flight at an altitude of two feet.

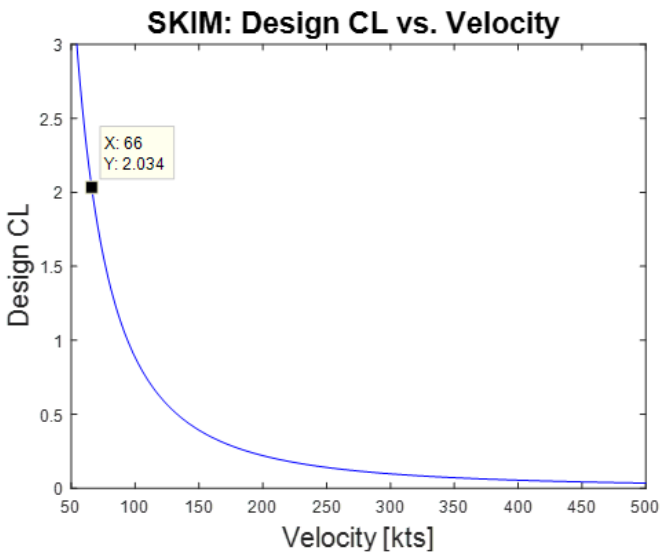

Landing Skim Speed @ 2 feet = 66 knots (76 mph)

Figure 57: Landing Speed in Skim at Two Feet Ground Effect Height for Reverse Delta with 10□ Anhedral Fixed Wing Configuration

The main design factor for the SUAV was the design speed in cruise and skim flight. The landing speed was also a design factor, but was only required to be of reasonably low magnitude. The main advantage of the Rectangular wing with 20° anhedral was the high lift coefficient values for low landing and loiter speeds. The Reverse Delta wing with 10° anhedral was selected as the ideal wing configuration to achieve optimum performance in both cruise and skim flight conditions because it achieved significantly higher flight speeds between the two wing configurations and still achieved reasonably low landing and loiter speeds. Table 5 displays the achievable flight speeds for the Reverse Delta wing with 10□ anhedral configuration concept.

Table 5: Achievable Flight Speeds for the Selected Fixed Wing Concept

Selected Wing Configuration: Reverse Delta with 10^0 Anhedral		
Performance Characteristics	**knots**	**mph**
Maximum Speed in Cruise	379	436
Maximum Speed in Skim at Five Feet	258	297
Maximum Speed in Skim at Two Feet	200	230
Minimum Loiter Speed in Cruise	122	140
Minimum Landing Speed in Skim at Five Feet	79	90
Minimum Landing Speed in Skim at Two Feet	66	76

The selected wing configuration concept, a Reverse Delta wing with 10° anhedral, satisfied the high flight speed requirement with a cruise speed of 379 knots, a skim speed of 258 knots at a five foot altitude, and a skim speed of 200 knots at a two foot altitude. With the help of high-lift devices, the concept is also capable of achieving reasonable landing speeds around 79 knots at a skim height of five feet and 66 knots at a skim height of two feet.

3.9 Aspect Ratio Trade Study

Having selected the wing configuration, the next step to determining the ideal shape of the wing for optimal performance in cruise and skim flight was to identify the corresponding aspect ratio. In order to determine the ideal aspect ratio, three aspect ratio variations of the Reverse Delta wing with 10□ anhedral were created. The aspect ratios tested were 2.34, 3.37, and 6. The first two values were selected to model the low aspect ratios in the range traditionally used for ground effect aircraft. These aspect ratios were close in value since the ideal aspect ratio was projected to be closer to that of a ground effect wing. A medium aspect ratio of 6, traditionally used on high speed subsonic aircraft was also tested. In selecting the aspect ratios to examine, the surface area and taper ratio for the wings were held constant, while it was the root chord length that was varied. Figure 58 depicts the three wings tested in XFLR5.

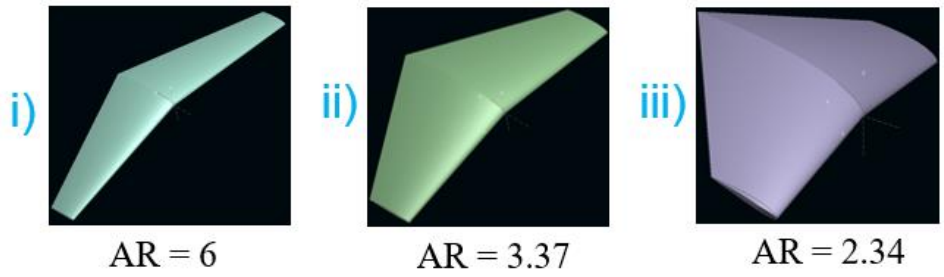

Figure 588: Aspect Ratio Variations of the Selected Reverse Delta with 10□ Anhedral Fixed Wing Concept

Similar to the comparison of the three final wing configuration concepts, the lift coefficients and moment coefficients were analyzed for each aspect ratio variation of the wing. Figure 59 shows the moment coefficient plots for the three wing aspect ratios.

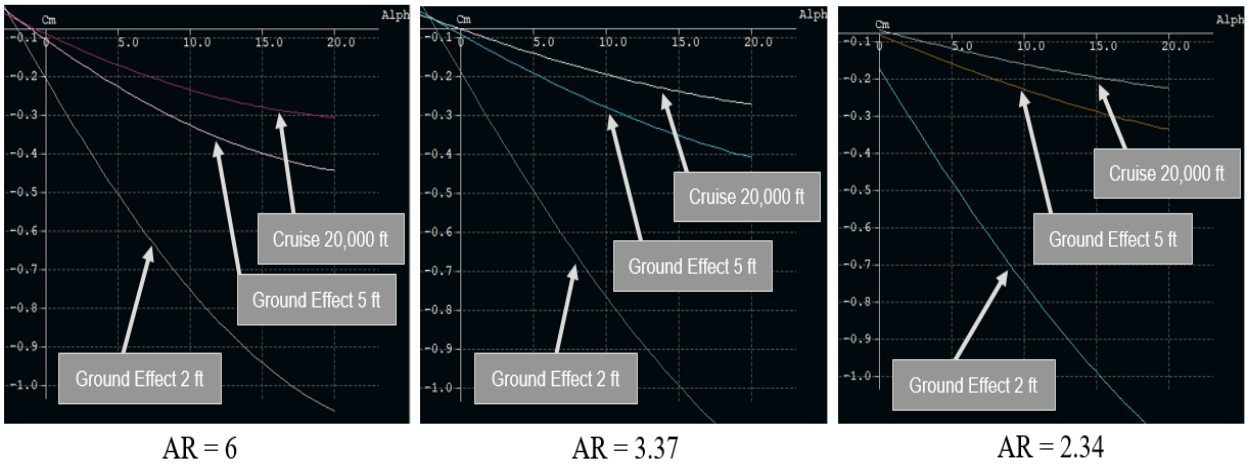

Figure 59: Moment Curves for the Aspect Ratio Variations of the Selected Reverse Delta with 10□ Anhedral Fixed Wing Concept

From these moment coefficient plots, it was identified that the aspect ratio does not affect the magnitude of the moment coefficients at their respective angles of attack. Instead, it is the surface area of the wing that influences the moment coefficient. Figure 61 exhibits the moment comparison for two Reverse Delta wings with 10□ anhedral. One wing has a surface area of 140 sq-ft and the other has a surface area of 267 sq-ft.

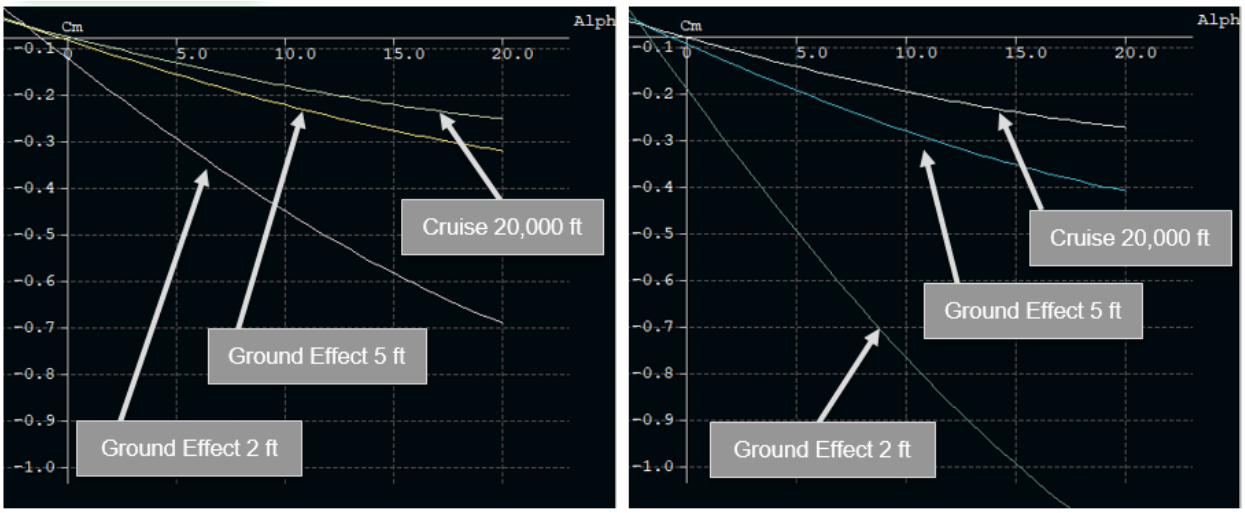

Figure 60: Wing Surface Area Influence on Moment Coefficients

From Figure 61, it was determined that as the surface area of the wing increases, so does the moment coefficient. Therefore, the moment coefficients were not a factor in determining the ideal aspect ratio for the wing.

The lift coefficients were then analyzed for the three wing aspect ratios. Figure 62 provides the lift coefficient data for the three aspect ratios at the angles of attack from 0□ to 20□.

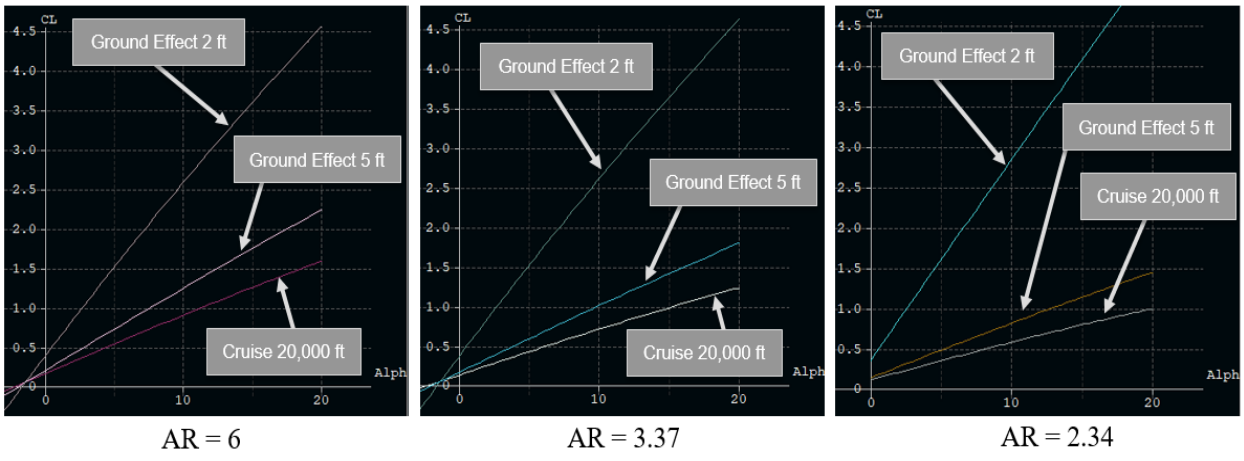

Figure 61: Lift Curve Slopes for Aspect Ratio Variations of the Selected Reverse Delta with 10□ Anhedral Fixed Wing Concept

Figure 62 shows that the differing aspect ratios only slightly change the magnitude of the lift coefficient values.

To get a better idea of the achievable lift coefficients of the three different aspect ratios in Figure 58, Figure 63 was created to provide a magnified view of the minimum achievable lift coefficient values at low angles of attack from 0° to 1° in the three flight conditions.

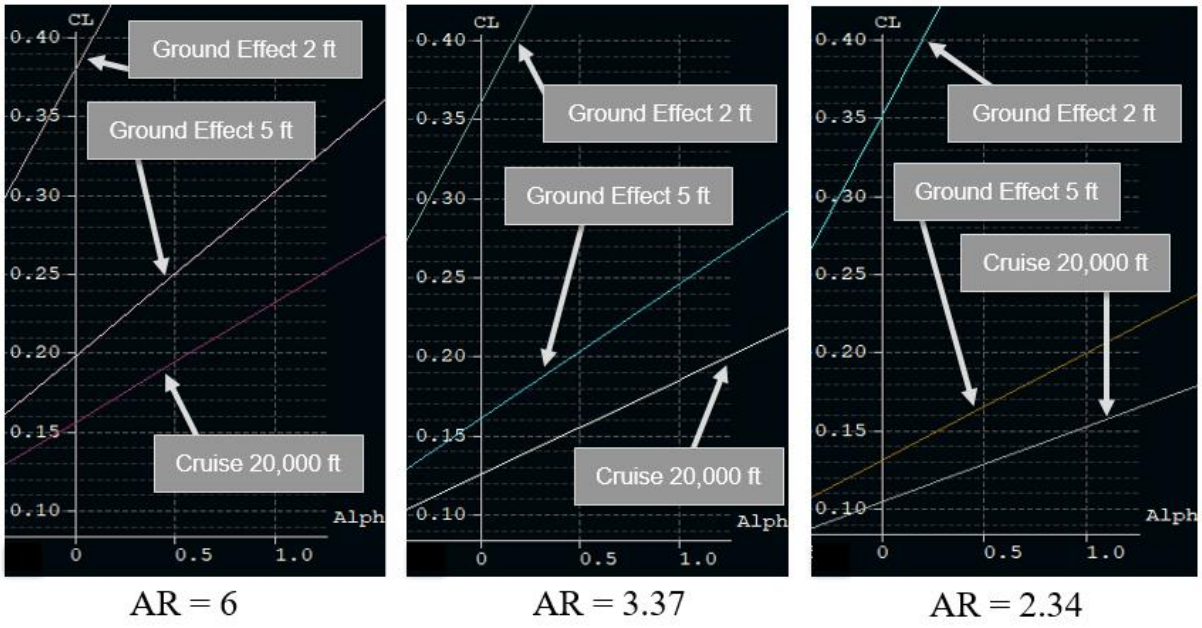

Figure 62: Lift Curve Slopes from 0° to 1° Angle of Attack for Aspect Ratio Variations of the Selected Reverse Delta with 10° Anhedral Fixed Wing Concept

Figure 63 shows that as the aspect ratio decreases, the minimum lift coefficients at 0° angle of attack decrease for all flight conditions. Therefore, the lower the aspect ratio of the wing, the greater the attainable cruise and skim velocities.

Figure 64 provides a magnified view of the maximum lift coefficients at 10° to 15° angle of attack achieved for the three different wing aspect ratios in the three flight conditions.

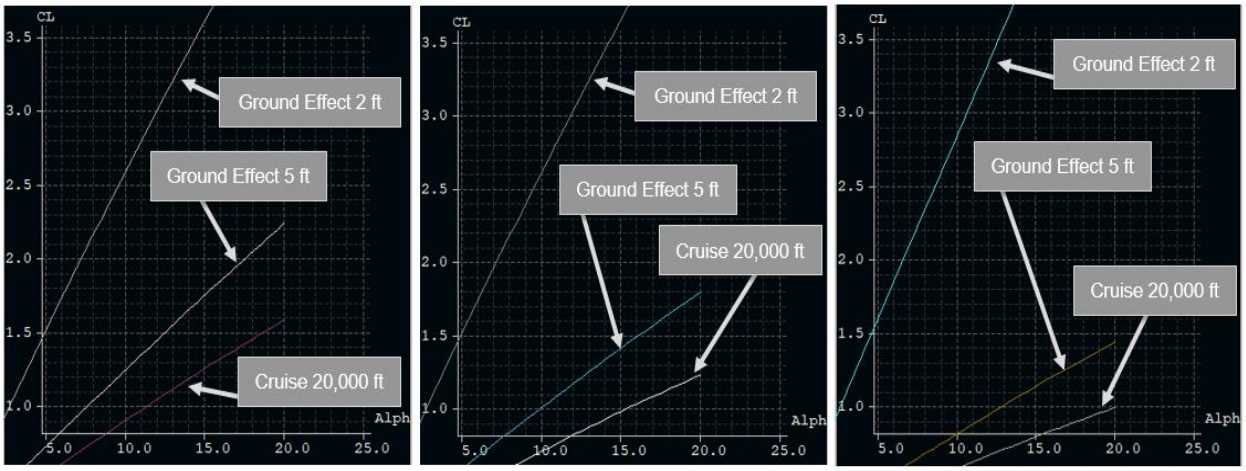

Figure 63: Lift Curve Slopes from 10□ to 20□ Angle of Attack for Aspect Ratio Variations of the Selected Reverse Delta with 10□ Anhedral Fixed Wing Concept

Figure 64 shows that decreasing the aspect ratio also decreases the maximum attainable lift coefficients, which transitively increases the value of the minimum achievable landing speed of the aircraft.

Since the aspect ratio of 3.37 achieves both low lift coefficients at 0° angle of attack and high lift coefficients at high angles of attack, it was selected as the ideal aspect ratio to achieve the best performance in both the cruise flight and skim flight conditions of the three aspect ratios examined. In general, the combination of the Reverse Delta wing with 10° anhedral configuration with the low aspect ratio around the value of three was selected for its ability to achieve high speed cruise flight, high speed skim flight, low loiter speeds in cruise, and low landing speeds in skim.

Chapter 4: SUAV Concept

4.1 Initial SUAV Configuration Concept

From the identification of a wing configuration and aspect ratio capable of optimum performance in both medium-altitude cruise flight and ground-effect skim flight, a rough initial concept for the submersible unmanned aerial vehicle was created. Figure 65 displays an isometric view and a three view of the initial SUAV concept.

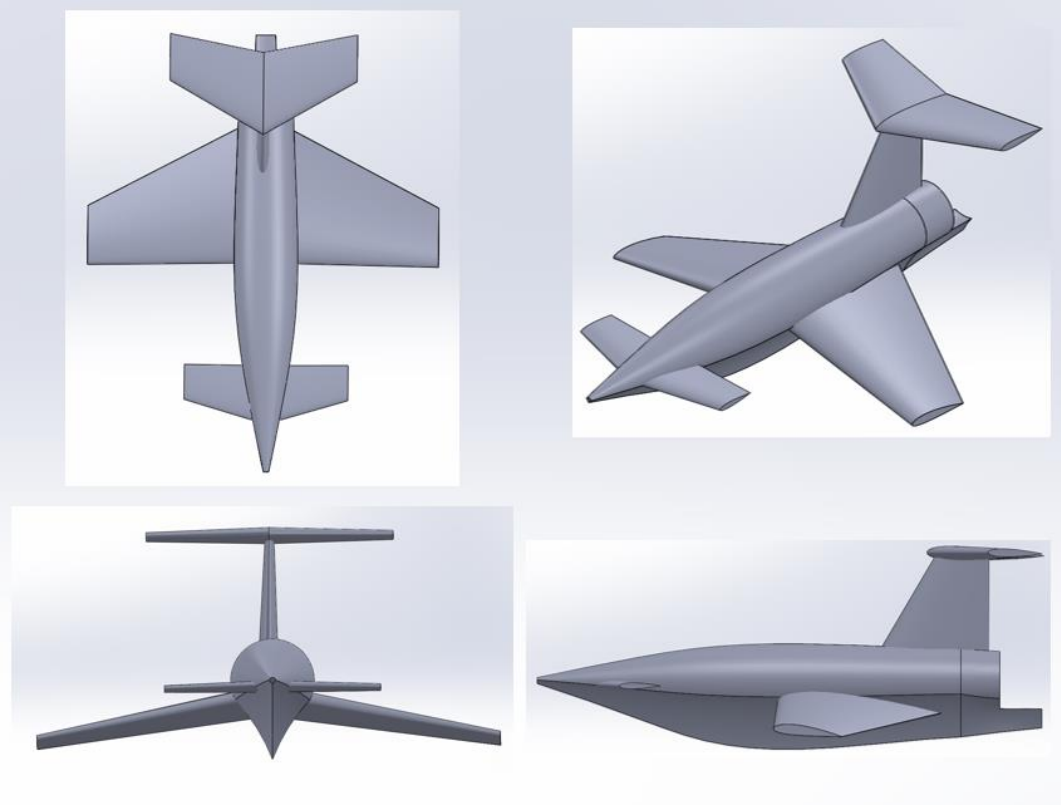

Figure 64: Isometric View of Initial SUAV Configuration Concept

The high T-tail configuration was selected for the initial concept due to its lightweight construction and increased horizontal tail effectiveness. The increased effectiveness of the horizontal tail assists in balancing the large moments experienced in ground-effect flight. A control canard was added to the nose of the aircraft to reduce the overall size of the horizontal tail, to reduce trim drag, and to help compensate for the losses of horizontal tail effectiveness experienced at higher angles of attack, where the tail

approaches deep stall conditions. However, the aircraft should never reach deep stall conditions since the canard is designed to stall first in order to ensure that the wing never stalls and that the aircraft never experiences a nose down moment. Both the control canard and horizontal tail were equipped with symmetric airfoils to enable them to create the positive and negative moments necessary for longitudinal stability in both cruise and skim flight. Figure 66 displays how the stabilizing surfaces balance the moments experienced in each flight condition.

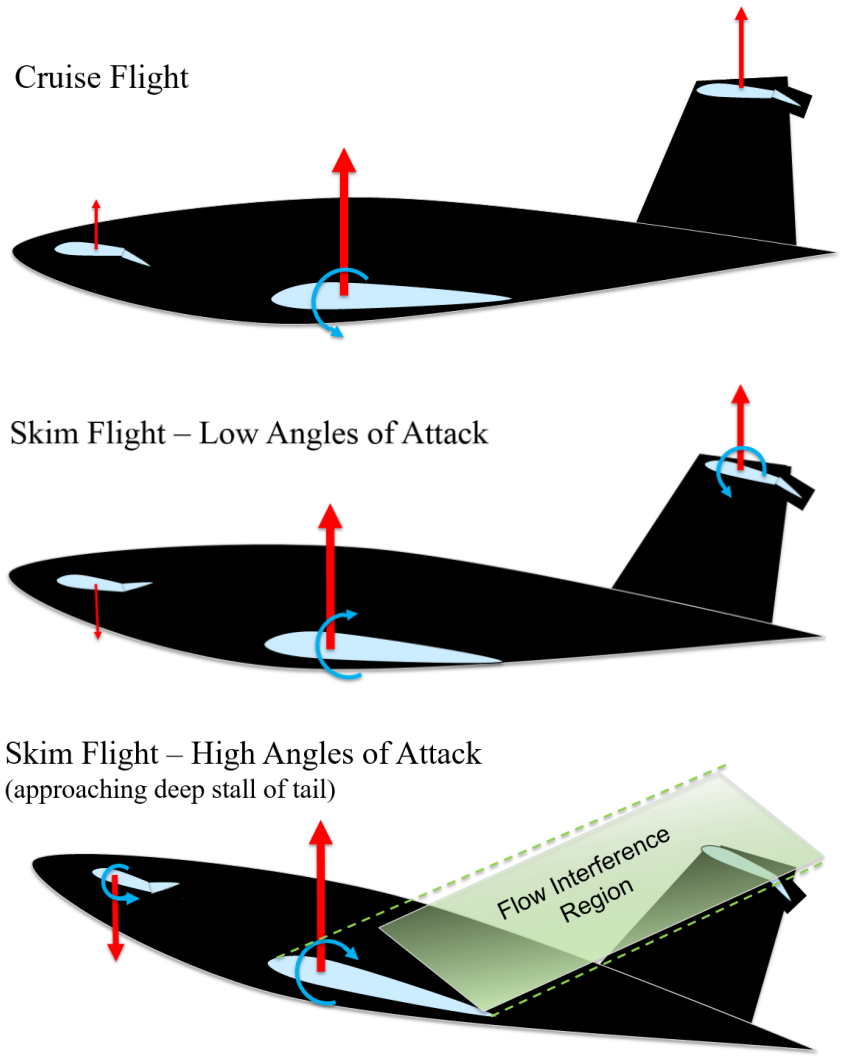

Figure 65: Stabilizing Lift Force Diagram for Wing in Cruise (TOP), in Skim at Low Angles of Attack (MIDDLE), and in Skim at High Angles of Attack (BOTTOM)

4.2 SUAV Functionality

The forward and aft main ballast tanks (MBT) are flooded in order to submerse the vehicle. Additional portions of the vehicle such as the wings, canard, tail structures, hull, and expendable payload bay are also flooded to reduce the required size of the MBT's. During the submersion process, the engine is sealed off in the pressure hull and the inlet ducts are flooded. Longitudinal stabilization while submersed is achieved with the flooding of the forward and aft trim tanks. The SUAV surfaces by using tanks of compressed air stored in the pressure hull to blow water from the flooded main ballast tanks. An expendable payload bay is located in the hull of the vehicle and only engaged while submersed. Figure 67 depicts the pressure hull, expendable payload bay, trim tanks, and main ballast tanks used for underwater operation.

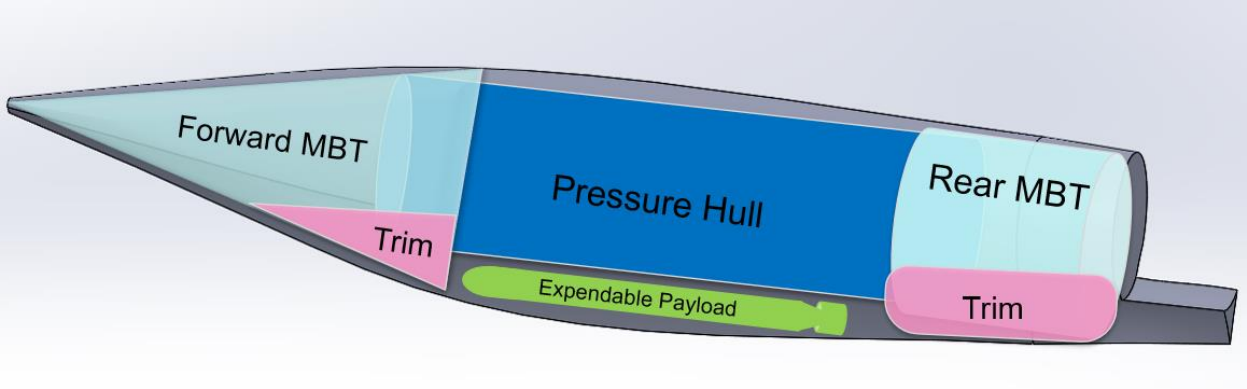

Figure 66: Floodable Fuselage Sections for Underwater Operations of SUAV

Much like the Convair F2Y Sea Dart, the SUAV lands on two retractable, forward-mounted hydro-skis and the aft hull portion of the fuselage. Figure 68 depicts the SUAV concept with hydro-skis extended.

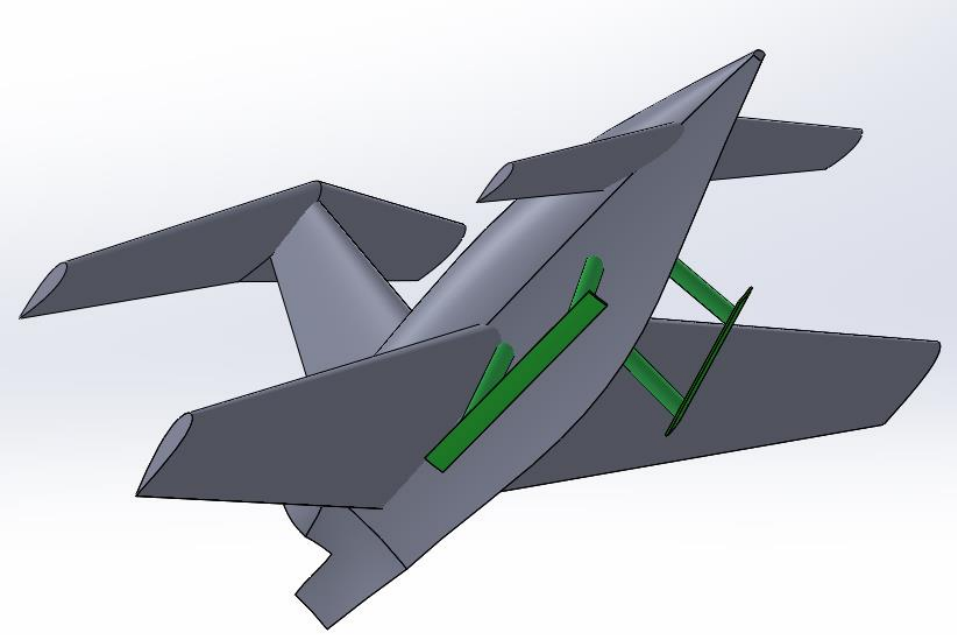

Figure 67: Landing Configuration for SUAV

In cruise and skim flight, the SUAV is powered by a single, low-bypass turbofan engine. In underwater operation, the vehicle is driven by a propeller connected to a battery-powered electric motor. Figure 69 displays a rough approximation of the internal layout of the pressure hull components.

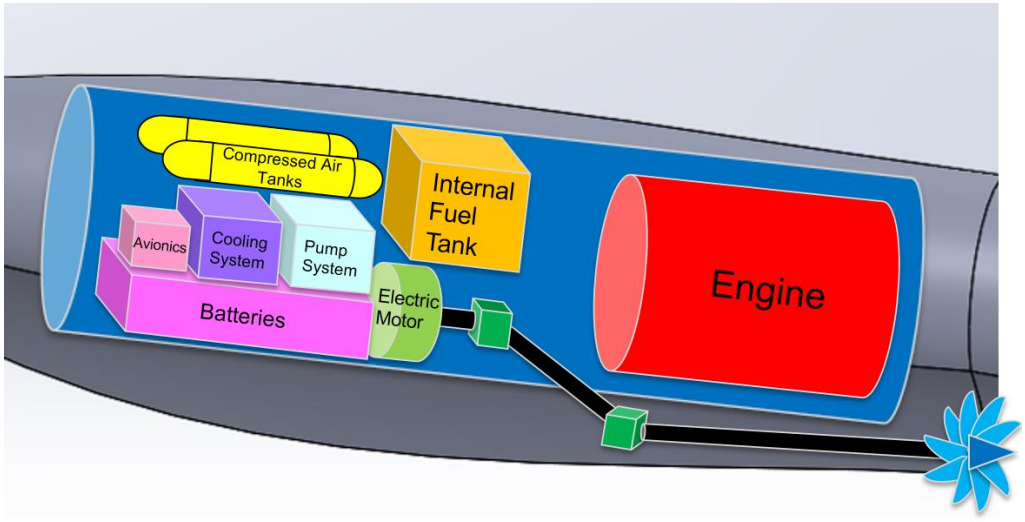

Figure 68: Internal Component Layout within Pressure Hull of SUAV

Although this is an initial configuration design concept, it does provide an opportunity to examine some of the main components necessary to accomplish the defined mission. It also offers solutions to major

challenges associated with a vehicle capable of both medium-altitude cruise flight and low-altitude skim flight.

Chapter 5: Conclusion

5.1 Wing Configuration Trade Study Results

The purpose of this research was to identify the ideal wing shape for a submersible unmanned aerial vehicle concept. This research analyzed morphing wing configurations for the ability to meet desired performance characteristics in both medium-altitude cruise flight and ground-effect skim flight. The desired performance characteristics of the wing included subsonic flight speeds equal to or greater than 333 knots (383 mph) in cruise, subsonic flight speeds equal to or greater than 200 knots (230 mph) in skim, loiter speeds equal to or less than 130 knots (150 mph) in cruise, and landing speeds equal to or less than 83 knots (96 mph) in skim. The lift and moment coefficients were identified as the main variables influencing the performance characteristics of the wing. Low lift coefficients correlated to higher flight speeds, while higher lift coefficients correlated to lower flight speeds. The moment coefficients associated with these lift coefficients were examined due to their abnormally high magnitudes and strong influence on the size of the horizontal tail. Therefore, the selected wing shape had to be capable of achieving both low lift coefficients at 0° angle of attack and high lift coefficients at 10° to 20° angle of attack in the cruise and skim flight conditions.

With the computational fluid dynamics software, XFLR5, four morphing wing configurations were analyzed in cruise flight at an altitude of 20,000 feet, in skim flight at a ground-effect height of five feet, and in skim flight at a ground effect height of two feet. The morphing wing configurations utilized either variable wing sweep or variable wing anhedral to achieve the desired performance metrics. The results of the wing analysis identified that of the morphing concepts, the configurations with variable anhedral increased the ability of the wings to achieve improved flight performance in both cruise and skim conditions the most. However, non-morphing versions of the configurations proved to be equal or better at meeting the desired performance characteristics. Therefore, three fixed wing configurations with anhedral were analyzed for the potential to meet the desired performance metrics. From the three

configurations analyzed, the Reverse Delta wing with 10° anhedral configuration proved the most capable of meeting the desired performance characteristics.

5.2 Aspect Ratio Trade Study Results

To further enhance the understanding of the ideal wing shape capable of meeting the desired performance metrics for a SUAV, an aspect ratio trade study was performed. The study examined the Reverse Delta wing with 10° anhedral configuration at three different aspect ratios in the cruise and skim flight conditions. The results showed that of the values tested, an aspect ratio of roughly three offered the highest potential for meeting the desired performance metrics. Moving forward, more wing trade studies will be performed to continue honing in on the optimum shape for a wing capable of meeting all of the desired performance metrics.

5.3 Initial SUAV Configuration Concept

The initial vehicle concept presented in chapter four offers an introduction to potential configurations for a submersible unmanned aerial vehicle. It serves as a brief overview for the components and operations necessary to accomplish missions involving medium altitude flight, low-altitude flight, and underwater navigation. Further trade studies, like the wing study performed in chapter three, are required to continue shaping such a vehicle. Once the flight performance metrics are met, submersion and underwater navigation research must begin. Although formidably challenging, the creation of a vehicle capable of flight and underwater operation is not impossible.

References

[1] Avionics Department Code, 450000E, Naval Air Warfare Center Weapons Division, Point Mugu, California. *Electronic Warfare and Radar Systems Engineering Handbook*. 4th ed., NAWCWD Technical Communication Office, 2013. *Defense Technical Information Center*. Web. 10 Oct. 2017.

[2] "Air velocity & pressure." *Omer Wing-Sail Ltd*. Seoweb, Web. 11 Nov. 2017. http://www.omerwingsail.com/air-velocity-pressure/

[3] De Keyser, Luc. "Ground Effect Vehicles: Adopting an Orphaned Technology." *Worldview*. Stratfor Enterprises, 08 July 2015. Web. 12 Nov. 2017.

[4] Ury, Allen B. "Ushakov LPL Flying Submarine (1934)." *Concept Aircraft*. Fantastic Plastic, 2010. Web. 14 Nov. 2017. http://fantastic-plastic.com/Ushakov_LPL_Flying_Sub_Page.htm

[5] Klein, Bernhard. "Bernhard C.F. Klein Collection No. 6559. Reid RFS-1 (N1740)." *1000aircraftphotos.com*. Webpotential, 18 June 2007. Web. 14 Nov. 2017.

[6] Anderson Jr., J.D. *Fundamentals of Aerodynamics*. 5th ed., Boston: McGraw-Hill, 2010. Print.